DIPARTIMENTO DI MATEMATICA
"Francesco Brioschi"
POLITECNICO DI MILANO

A new mathematical explanation of the Tacoma Narrows Bridge collapse

Arioli, G.; Gazzola, F.

Collezione dei *Quaderni di Dipartimento*, numero **QDD 149**
Inserito negli *Archivi Digitali di Dipartimento* in data 22-3-2013

Piazza Leonardo da Vinci, 32 - 20133 Milano (Italy)

A new mathematical explanation of the Tacoma Narrows Bridge collapse

Gianni ARIOLI [♯] - Filippo GAZZOLA [†]

[♯] MOX– Modellistica e Calcolo Scientifico
[♯,†] Dipartimento di Matematica – Politecnico di Milano
Piazza Leonardo da Vinci 32 - 20133 Milano, Italy
gianni.arioli,filippo.gazzola@polimi.it

Abstract

The spectacular collapse of the Tacoma Narrows Bridge, which occurred in 1940, has attracted the attention of engineers, physicists, and mathematicians in the last 70 years. There have been many attempts to explain this amazing event. Nevertheless, none of these attempts gives a satisfactory and universally accepted explanation of the phenomena visible the day of the collapse.

The purpose of the present paper is to suggest a new mathematical model for the study of the dynamical behavior of suspension bridges which provides a realistic explanation of the Tacoma collapse.

1 Introduction

1.1 The Tacoma Narrows Bridge collapse

The collapse of the Tacoma Narrows Bridge (TNB), which occurred on November 7, 1940, is certainly the most celebrated structural failure of history both because of the impressive video [44] and because of the huge number of studies that it has generated. However, after more than seventy years, a full explanation of the reasons of the collapse is not available. In particular, although many partial answers were given, up to nowadays there is no satisfactory unanimously shared answer to the main question:

why did torsional oscillations appear suddenly? (**Q**)

The TNB was considered very light and flexible. Not only this was apparent to traffic after the opening, but also it was felt during the construction. According to [39, pp.46-47], *...during the final stages of work, an unusual rhythmic vertical motion began to grip the main span in only moderate winds ... these gentle but perceptible undulations were sufficient to induce both bridgeworker nausea and engineering concern*. The undulatory motion of the span attracted the local interest and *...motorists ventured onto the TNB to observe vehicles ahead of them slowly disappearing in the trough of a wave*. So, it was not surprising that vertical oscillations were visible on the day of the collapse. The wind was blowing at approximately 80 km/h and, apparently, *the oscillations were considerably less than had occurred many times before*, see [39, p.49]. Hence, although the wind was the strongest so far since the bridge had been built, the motions were in line with what had been observed earlier. However, a sudden change in the motion was alarming. Without any intermediate stage, a violent destructive torsional movement started: the oscillation changed from nine or ten smaller waves to the two dominant twisting waves. A witness to the collapse was Farquharson, the man escaping in the video [44]. According to his detailed description [11] *...a violent change in the motion was noted. This change appeared to take place without any intermediate stages and with such extreme violence that the span appeared to be about to roll completely over*.

Leon Moisseiff (1873-1943), who was charged with the project, had an eye to economy and aesthetics, but he was not considered guilty for the TNB failure. For instance, Steinman-Watson [43] wrote that *...the span failure is not to be blamed on him; the entire profession shares in the responsibility. It is simply that the profession had neglected to combine, and apply in time, the knowledge of aerodynamics and of dynamic vibrations with its rapidly advancing knowledge of structural design*. The reason of this discharge probably relies on forgotten similar collapses previously occurred. For instance, one should compare the torsional motion prior to the collapse of the Brighton Chain Pier in 1836, as painted by William Reid [34, p.99], and torsional motions prior to the TNB collapse, see Figure 1.

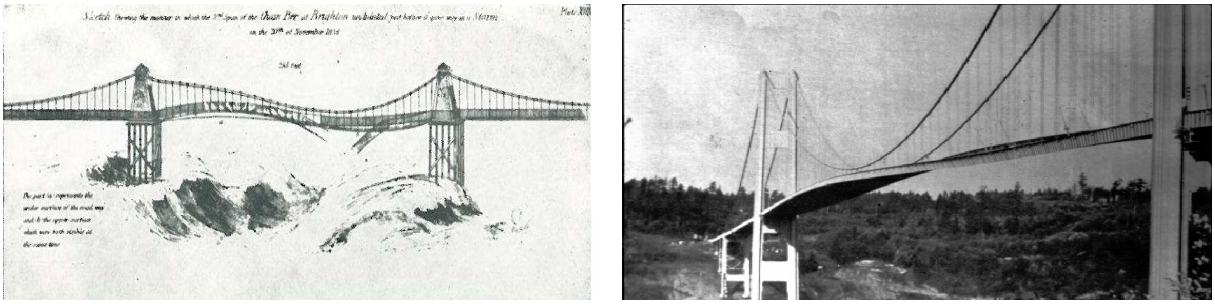

Figure 1: Torsional motion in the Brighton Chain Pier and in the Tacoma Narrows Bridge.

Similar torsional behaviors were displayed in several other bridges before 1940, see [39, Section 4.3], [22, p.75], and also [14, Section 2]. So, it seems that torsional oscillations are to be expected in flexible suspension bridges. Still, the natural questions which arise from the TNB collapse and from similar failures are the following [39, p.53]:
- how could a span designed to withstand 161 km/h winds and a static horizontal wind pressure of 146 kg/m^2 succumb under a wind of less than half that velocity imposing a static force one-sixth the design limit?
- how could horizontal wind forces be translated into dynamic vertical and torsional motion?

In fact, the answers to these questions are strictly linked. The bridge was ready to withstand 161 km/h wind provided that the oscillation would have been longitudinal. But since unexpected torsional oscillations appeared, this considerably lowered the critical speed of the wind. Therefore, the two above questions reduce to the main question **(Q)**.

Soon after the TNB accident three engineers were assigned to investigate the collapse and report to the Public Works Administration: O.H. Ammann, T. von Kármán, and G.B. Woodruff. Their Report [1] contains several answers to minor questions such as technical details on the project and comments on the flexibility. The Report considers *...the crucial event in the collapse to be the sudden change from a vertical to a torsional mode of oscillation*, see [39, p.63]. However, no convincing response to **(Q)** appears and several conclusions of the Report raised criticisms. Since then, many different attempts to answer to **(Q)** have been made. Some explanations attribute the failure to a structural problem, some others to the resonance between the exterior wind and the oscillating modes of the bridge. Further explanations involve vortices, due both to the particular shape of the bridge and to the angle of attack of the wind. Finally, let us mention explanations based on flutter theory and self-excited oscillations due to the flutter speed of the wind. In the Appendix we discuss in detail all these theories and we explain why they fail to answer satisfactorily to **(Q)**.

1.2 Previous mathematical models

The celebrated report by Navier [31] has been for about one century the only mathematical treatise of suspension bridges. The second milestone contribution is certainly the monograph by Melan [29]. After the TNB collapse, the scientific community felt the necessity to find accurate equations in order to attempt explanations of what had occurred. In this respect, historical sources are [8, 40] which consider the function representing the amplitude of the vertical oscillation as unknown but do not consider torsional oscillations.

In a model suggested by Scanlan-Tomko [38], the angle of twist α of the torsional oscillator (bridge deck section) is assumed to satisfy the equation

$$I\left[\ddot{\alpha} + 2\zeta_\alpha \omega_\alpha \dot{\alpha} + \omega_\alpha^2 \alpha\right] = A\dot{\alpha} + B\alpha \,, \tag{1}$$

where I, ζ_α, ω_α are, respectively, associated inertia, damping ratio, and natural frequency. The aerodynamic force (the r.h.s. of (1)) is assumed to depend linearly on both $\dot{\alpha}$ and α with the positive constants A and B depending on several parameters of the bridge. Constant coefficient second order linear equations such as (1) have elementary solutions. Roughly speaking, one can say that chaos manifests itself as an unpredictable behavior of the solutions in a dynamical system. With this characterization, there is no doubt that chaos was somehow present in the dynamic of the TNB. From [18, Section 11.7] we recall that *neither linear differential equations nor systems of less than three first-order equations can exhibit chaos*. Since (1) may be reduced to a two-variables first order linear system, it cannot be suitable to describe the disordered behavior of the bridge and fails to explain the sudden appearance of torsional oscillations that contemporaneously changed the vertical oscillations ...*which a moment before had involved nine or ten waves, had shifted to two*, as described by Farquharson [11]. In order to have a more reliable description of the bridge, the fourth order nonlinear ODE $w'''' + kw'' + f(w) = 0$ ($k \in \mathbb{R}$) was studied in [5, 15, 16, 17]: solutions to this equation blow up in finite time with self-excited oscillations appearing suddenly, without any intermediate stage, see [17].

In [9, 14] one may find strong evidence that some nonlinearity should be involved. That linearization yields wrong models is also the criticism by McKenna [26, p.4], who comments (1) by writing *This is the point at which the discussion of torsional oscillation starts in the engineering literature*. He claims that the problem is in fact nonlinear and that (1) is obtained after an incorrect linearization; we come back to this delicate point a few lines below. McKenna concludes by noticing that *Even in recent engineering literature ... this same mistake is reproduced*. In fact, any model aiming to describe the complex behavior of a bridge has to face a difficult choice between accurate but complicated equations on one hand and simplified but less reliable equations on the other hand. We refer to [14, Section 3.2] for a detailed story of further mathematical models which, unfortunately, could not lead even to partial answers to **(Q)**.

In order to view torsional oscillations, McKenna [26] makes a breakthrough by considering the cross section of the roadway as a rod having four degrees of freedom. The first two degrees of freedom are the downwards vertical displacement y of its center B with respect to equilibrium and its velocity $\dot{y}$, whereas the other two degrees of freedom are the angle of deflection from the horizontal position θ and the angular velocity $\dot{\theta}$. The rod is hanged at its endpoints by two springs C_1 and C_2, as in Figure 2.

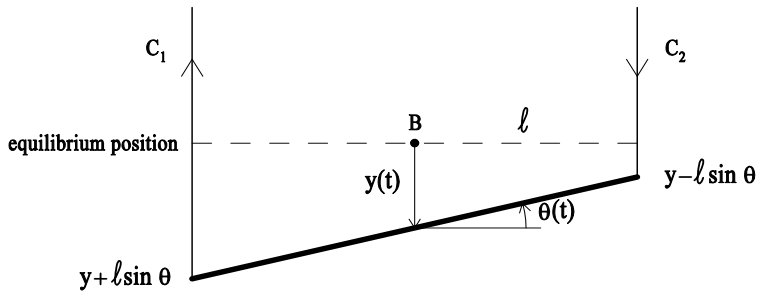

Figure 2: Vertical (y) and torsional (θ) displacements of a cross section of the bridge.

The rod, having mass m and length 2ℓ, is free to rotate about its center with angular velocity $\dot{\theta}$ and therefore has a kinetic energy given by $m\ell^2\dot{\theta}^2/6$. Moreover, the center B of the cross section behaves as a forced oscillator where the forces are exerted by the two lateral hangers C_1 and C_2, and are denoted respectively by $f(y + \ell\sin\theta)$ and $f(y - \ell\sin\theta)$; these terms should also take into account the negative

gravity force. Summarizing, the system describing the vertical-torsional oscillations of the rod is

$$\frac{m\ell^2}{3}\,\ddot{\theta} = \ell\cos\theta\,\Big(f(y-\ell\sin\theta) - f(y+\ell\sin\theta)\Big)\,, \quad m\,\ddot{y} = -\Big(f(y-\ell\sin\theta) + f(y+\ell\sin\theta)\Big)\,, \quad (2)$$

where θ represents the angle of deflection of the cross section from horizontal, y the downwards displacement of the barycenter B from equilibrium, m is the mass of the rod modeling the roadway section, 2ℓ its width. The delicate point is the choice of the restoring force f which McKenna [26] takes as $f(s) = (s+1)^+ - 1$ and justifies this choice by considering the hangers as linear springs which may slacken if the roadway has large upwards deflections: when the hangers are stretched there is a restoring force which is proportional to the amount of stretching, but when the cross section moves in the opposite direction there is no restoring force exerted on it and the only force acting is gravity. Here, s denotes the vertical displacement of an endpoint of the cross section. When $s = 0$ the considered endpoint is in equilibrium, namely the upwards positive restoring force due to the hanger has exactly the same strength as the downwards negative gravity force and therefore the total force vanishes. When $s < 0$ (recall that negative s are upwards) the endpoint is above equilibrium and therefore the gravity force is stronger than the restoring force and hence the total force is negative, that is, oriented downwards. There is a limit position, say $s = -1$, where the hanger slackens; therefore, for $s \le -1$ there is no restoring force and the endpoint is merely subject to gravity which is normalized to -1. Subsequently, in order to smoothen the force by maintaining the asymptotically linear behavior as $s \to 0$, McKenna-Tuama [28] take the alternative form $f(s) = e^s - 1$.

According to [26], a key error in previous models was the linearization of (2) with respect to θ, the term $\sin\theta$ was usually replaced by θ whereas $\cos\theta$ was replaced by 1. This is reasonable for small θ, but appears inaccurate for large deflections. So, a major point, also known among engineers [9], is that excessive linearizations may lead to inaccurate models (such as (1)) and to unreliable responses. And indeed, [26, Section 3.1] shows that numerical solutions to (2) starting with large initial data die down in the linear model while they do not for the nonlinear model where large oscillations continue for all time until the eventual collapse of the bridge: by linear model we mean here that the approximation $\sin\theta \approx \theta$ is made, whereas nonlinear means that $\sin\theta$ is maintained. In these experiments the restoring force is assumed to be piecewise linear. In our opinion, although the approximation $\sin\theta \approx \theta$ is inaccurate, it does not hide the main phenomenon (see Section 3.1), while we believe that the nonlinearity in the restoring force f plays the major role. By no means, for large displacements one can apply the linear Hooke law of elasticity. This is also the opinion of McKenna [26, p.16]: *We doubt that a bridge oscillating up and down by about 10 meters every 4 seconds obeys Hooke's law*. Using the above model (2), [26, 28] were able to numerically replicate in a cross section the most mysterious and unexplained phenomenon observed at the TNB, namely the sudden transition from somehow standard and expected vertical oscillations to the destructive and unexpected torsional oscillations. They found that, if the vertical motion was sufficiently large to induce brief slackening of the hangers, then numerical results highlighted a rapid transition to a torsional motion. It was however pointed out by the physicists Green-Unruh [19] that a report by Farquharson in [1] states that ...*the riser cables were not slack during the oscillation*. If this were true, then the forcing term f would be linear. And linear restoring forces f do not allow an answer to **(Q)**. On the other hand, as we have just written above, the linear law of elasticity is just an approximation of the full nonlinear law and can be used only for small oscillations. As we shall see, any apparently harmless tiny nonlinear perturbation of linear forces yields the possibility of a sudden switch from vertical to torsional oscillations in the model system (2).

No model is perfect and, for sure, it may be improved. By commenting the results in [26, 28], McKenna-Moore [27, p.460] write that ...*the range of parameters over which the transition from vertical to torsional motion was observed was physically unreasonable ... the restoring force due to the cables was oversimplified ... it was necessary to impose small torsional forcing*. The latter kind of forces were observed in wind tunnel experiments [38] and may also be justified by the Larsen theory [23] with nonconstant angles of attack of the wind, see Section 5.3. But a further remark in [27] is of crucial importance for our purposes, namely that *the torsional oscillations that preceded the collapse were never observed until the day of the collapse ... there is considerable historical evidence for the presence of vertical forcing, but no evidence of the type*

of periodic forces that we imposed... On the other hand, the collapse of the Brighton Chain Pier and other bridges, see Figure 1, displayed torsional oscillations. We will explain why torsional oscillations may be seen, or may be hidden, or may even not appear.

A model suggested by Moore [30] extends (2) to the entire length L of the roadway. Assuming again that the restoring forces are piecewise linear, the following generalization of problem (2) is obtained

$$\begin{cases} \theta_{tt} - \varepsilon_1 \theta_{xx} = \frac{3K}{m\ell} \cos\theta[(y - \ell \sin\theta)^+ - (y + \ell \sin\theta)^+] - \delta\theta_t + h_1(x,t) \\ y_{tt} + \varepsilon_2 y_{xxxx} = -\frac{K}{m}[(y - \ell \sin\theta)^+ + (y + \ell \sin\theta)^+] - \delta\theta_t + g + h_2(x,t) \\ \theta(0,t) = \theta(L,t) = y(0,t) = y(L,t) = y_{xx}(0,t) = y_{xx}(L,t) = 0 \,, \end{cases} \tag{3}$$

where ε_1, ε_2 are physical constants related to the flexibility of the beam, $\delta > 0$ is the damping constant, h_1 and h_2 are external forces, and g is the gravity acceleration. Multiple periodic solutions to (3) are determined in [30]. We believe that (3) is a nice reliable model which, however, may be improved in several aspects. First, the restoring force needs not to be piecewise linear; second, it does not act on the whole length of the roadway but only in those finite points where the hangers are present. Moreover, we feel that the answer to **(Q)** is hidden in a generalized version of system (2) independently of external forces. In this paper we suggest an alternative model which takes into account these remarks. It would be of great interest for engineers if a suspension bridge project could depend more on the non-random part of the model rather than on unpredictable external forces.

1.3 Purposes of the present paper

All the theories described in the Appendix have their own interest and cannot be entirely rejected even if none of them gives a satisfactory answer to **(Q)**. Precisely in order to give an answer to **(Q)**, we address a further question: did the TNB collapse because of a strong wind or because of some internal phenomenon not well understood? A first hint for an answer is given in the previously recalled remark from [39, p.53]: the TNB collapsed under a wind of less than half the security velocity and a static force one-sixth of the design limit. And a second hint is that, regardless of the name we give to the phenomenon (resonance, vortex street, flutter, etc...), it appears impossible that an *irregular* wind might generate a *regular* torsional oscillation. So, it seems that the explanation is not the behavior of the wind and this leads us to study more carefully what happens **inside the bridge**.

Although the theories in Section 5 differ as to what exactly caused the torsional oscillation of the bridge, they all agree that the extreme flexibility, slenderness, and lightness of the TNB allowed these oscillations to grow until they destroyed it. One of the purposes of the present paper is to put all together these explanations and to give a new mathematical description of what was observed the day of the TNB collapse. Our starting point is the McKenna model (2): the results obtained in [26, 28] are quite promising, these were the first papers able to reproduce the motion visible in [44]. However, we believe that the model may be improved in two crucial aspects.

A first crucial aspect is that the restoring force f in (2) should be nonlinear from the very beginning: also for small displacements one is not allowed to apply the linear Hooke law of elasticity. We already quoted several sources explaining why the phenomenon is nonlinear and, in our opinion, a piecewise linear force does not describe accurately the reality. Only in case of slackening hangers the piecewise linear force behaves nonlinearly. The legitimate doubt whether hangers indeed slackened the day of the TNB collapse is not the only contraindication to this kind of force. Then one should take a nonlinear perturbation of a linear force to be adapted to the real structure of the bridge and, in particular, to the elasticity of the hangers. This will not be discussed here in full detail, but will be the object of a forthcoming paper.

A second crucial aspect is the one previously mentioned: there is no explanation why an irregular wind should generate regular oscillations. Surely the wind does insert energy into the structure, thereby creating oscillations but, by no means, its behavior will determine the form of the oscillations. Hence,

the bridge behaves driven by its own internal features,
independently of the angle of attack and of the frequency of the wind.

In order to figure out what was the starting spark for torsional oscillations at the TNB, we get rid of all the "pollution contributions" which may hide the true phenomena. We strip the model and we consider a problem without any internal damping (friction) and any external forcing (wind or traffic load). The system we originally study is isolated and conserves energy, whence the initial conditions determine the total energy of the system. This enables us to show that the unsolved mystery, the sudden switch between vertical and torsional motions, is internal in the bridge structure. The cross section of the bridge acts as a double oscillator, whose components interact whenever the restoring force f is assumed to be nonlinear. In this case, the two oscillators (vertical and torsional) may **transfer energy**, meaning by this that wide oscillations of the first oscillator may suddenly decrease and generate wide oscillations of the second oscillator: although the total energy is conserved, some energy may transfer from one oscillator to the other. In Section 2 we show that the energy transfer, which is well displayed in Figure 4, may have a significant amplitude only above a critical energy threshold. With an abuse of language, we call these situations **internal resonance** which means that the two oscillators that compose the bridge have somehow compatible nonlinear frequencies and, therefore, can transfer a substantial amount of their oscillation amplitudes. The transfer of energy may occur suddenly, without any intermediate stage. Internal resonance depends on all the parameters of the model such as the explicit form of the nonlinearity f, the length of the cross section, and the nonlinear frequencies. For a given bridge all these parameters are fixed and then we show that internal resonance merely depends on the level of the total energy: only when the total energy is larger than some critical threshold one may observe a substantial energy transfer between the two oscillators. Such threshold strongly depends on the structure of the bridge, therefore we feel that an accurate comprehension of the phenomenon may lead to much sounder projects. And, hopefully, our results may give hints on how to plan future bridges in order to prevent destructive torsional oscillations without excessive costs for stiffening trusses.

In Section 2.2 we explain how to determine the critical energy level creating internal resonance in the cross section of the bridge. These levels are determined by analyzing the eigenvalues of the linearized Poincaré map (see e.g. [18, Section 11.5]) which is obtained by taking a section of the energy hypersurface. This analysis confirms the possibility of a sudden switch between the regime where the two oscillators behave almost independently and the regime where they transfer energy.

So far we merely considered a cross section which is free to oscillate both vertically and torsionally, see Figure 2. Next, we also consider the length of the bridge. Finding some analogies with a model previously studied by us [2, 3, 4] and also with the celebrated Fermi-Pasta-Ulam model [12], we consider a finite number of oscillators which are linked to the nearest neighbor with suitable restoring forces representing resistance to longitudinal stretching. This is a discretization of the bridge as if we were considering the toy bridge in Figure 3. Suspension bridges are indeed discrete structures since the hangers have positive

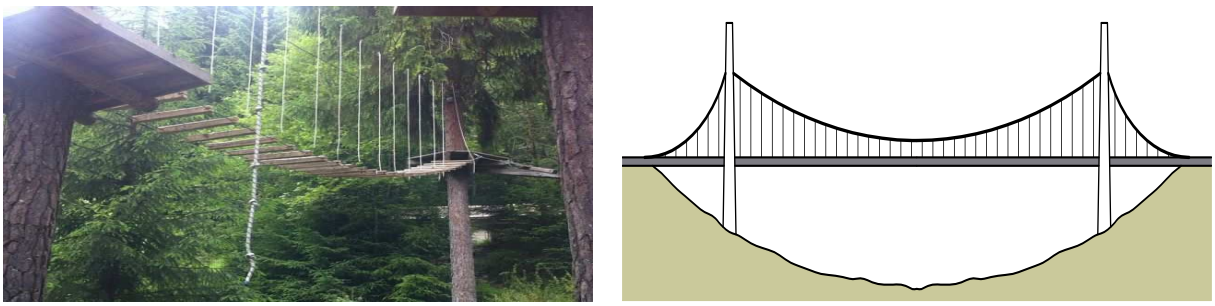

Figure 3: A toy bridge (left), possible discretization of a suspension bridge (right).

distance between each other, see again Figure 3, and the restoring forces to the equilibrium position act only on those cross sections linked to the hangers. We believe that, if one also considers the longitude of

the bridge, this discrete model is more realistic than (3). In Section 4 we exhibit some numerical results which, again, highlight a transfer of energy between vertical and torsional oscillations. A substantial energy transfer between oscillators occurs only at certain energy levels. Although this model has many degrees of freedom, these energy levels may be determined by analyzing the eigenvalues of the linearized Poincaré type maps. This model reproduces fairly well what was observed the day of the TNB collapse, see the experiments in Section 4. In order to confirm that the observed phenomenon is a satisfactory answer to **(Q)**, we add to the cross section model internal damping and external forcing, and we add damping to the model with n cross sections. As expected, damping terms tend to decrease the energy of the system and hence the width of the oscillations, whereas suitable external forces may increase the energy and the width of oscillations. Regardless of these modifications, the very same phenomenon remains visible: there is sudden energy transfer between the oscillators. Is this the final answer to **(Q)**?

This paper is organized as follows. In Section 2 we strip the McKenna double oscillator model and we show that there may be a sudden transfer of energy between oscillators; this transfer is justified by a careful analysis of suitable Poincaré maps in Section 2.2. In Section 3 we show that our results are robust, they do not qualitatively depend on the parameters involved. In Section 4 we describe the full bridge model and we show that energy transfer occurs within this model. Finally, in Section 4.4 we draw our conclusions and explain how our results may be used to give an answer to **(Q)** and to obtain suggestions for projects of future bridges.

2 A single cross section model

2.1 Quadratic perturbation of linear forces

The starting point of our analysis is the system (2) introduced by McKenna [26], which describes the cross section of the bridge as illustrated in Figure 2.

Note that if f is linear, then (2) decouples and describes two independent oscillators. We consider here a linear force with a quadratic perturbation, that is $f(s) = \alpha s + \beta s^2$ with $\alpha, \beta > 0$. This function should not be considered globally, but only for small values of s which represents the vertical displacement $y \pm \ell \sin\theta$ of an endpoint of the cross section, see again Figure 2. We performed several experiments and we observed that the values of the constants α and β do not modify the qualitative behavior of solutions. So, for our convenience, we take $f(s) = \frac{s+s^2}{2}$. In fact, the force we have in mind is

$$f(s) = \begin{cases} \frac{s+s^2}{2} & \text{if } s \geq -\frac{1}{2} \\ -\frac{1}{8} & \text{if } s \leq -\frac{1}{2} \end{cases} \tag{4}$$

and its graph is just "half parabola ended with an horizontal half line". This looks like a smooth version of the force $f(s) = (s+1)^+ - 1$ suggested by McKenna [26] with the important difference that f is nonlinear also for small s. Clearly, (4) is more similar to the force $f(s) = c(e^{as} - 1)$ subsequently considered in [28]. According to (4), when $s = 0$ the elastic force exerted by the hanger balances the gravity and the endpoint is at an equilibrium. The limit position where the hanger slackens is given by $s = -1/2$, so that for $s \leq -1/2$ there is no restoring force and the endpoint is merely subject to the gravity acceleration which has been rescaled to $g = \frac{1}{8}$.

Note also that, by the time scaling $t \mapsto \sqrt{m}t$, we can set $m = 1$ and we may rewrite (2) as

$$\begin{cases} \frac{\ell^2}{3}\ddot{\theta} + \frac{\partial U(\theta,y)}{\partial \theta} = 0 \\ \ddot{y} + \frac{\partial U(\theta,y)}{\partial y} = 0 \end{cases} \tag{5}$$

where

$$U(\theta, y) = F(y + \ell\sin\theta) + F(y - \ell\sin\theta) \qquad \text{and} \qquad F(s) = \int_0^s f(\tau)d\tau\,. \tag{6}$$

This yields an energy, invariant under the flow of (5), given by

$$\mathcal{E} = \frac{\ell^2\,\dot\theta^2}{6} + \frac{\dot y^2}{2} + U(\theta, y)\,. \tag{7}$$

When f is as in (4), as long as $y(t) \pm \ell \sin(\theta(t)) \geq -\frac{1}{2}$, (5) takes the simpler form

$$\begin{cases} \ddot\theta + 3\cos(\theta)\sin(\theta)(1+2y) = 0 \\ \ddot y + y + y^2 + \ell^2 \sin^2(\theta) = 0\,; \end{cases} \tag{8}$$

we consider a generic Cauchy problem

$$\theta(0) = \theta_0\,, \quad \dot\theta(0) = \theta_1\,, \quad y(0) = y_0\,, \quad \dot y(0) = y_1\,, \tag{9}$$

and observe that, if $\theta_0 = \theta_1 = 0$ and the couple (y_0, y_1) is sufficiently small, so that we are in the regime of (8), then the solution to (8)-(9) is given by $\theta(t) \equiv 0$ and by the unique (periodic) solution to

$$\ddot y + y + y^2 = 0, \quad y(0) = y_0\,, \quad \dot y(0) = y_1\,. \tag{10}$$

On the other hand, $y \equiv 0$ is a solution to (5) if and only if $\theta \equiv 0$; hence, in (5) the role of the two unknowns θ and y is quite different. Our purpose is to study the stability of the trivial solution $\theta \equiv 0$ when $(\theta_0, \theta_1) \neq (0,0)$ are small. To this end, we take initial data (9) with a given proportion, namely

$$(\theta_0, \theta_1) = 10^{-4}(y_0, y_1)\,. \tag{11}$$

This means that at $t = 0$ the torsional oscillations θ are negligible with respect to vertical oscillations y. By maintaining the proportion (11) we will see that the only parameter that influences the behavior of the system is its energy (7), and it does not matter how it is split between its kinetic and potential part.

Take $\ell = 1$; in Figure 4 we display the graphs of the solutions to

$$\begin{cases} \ddot\theta + 3\frac{\partial U(\theta,y)}{\partial \theta} = 0 \\ \ddot y + \frac{\partial U(\theta,y)}{\partial y} = 0\,, \end{cases} \qquad \dot\theta(0) = \dot y(0) = 0\,, \quad y(0) = y_0 = 10^4\theta(0)\,, \tag{12}$$

for different values of the parameter y_0. It appears clearly from Figure 4 that there is some energy transfer

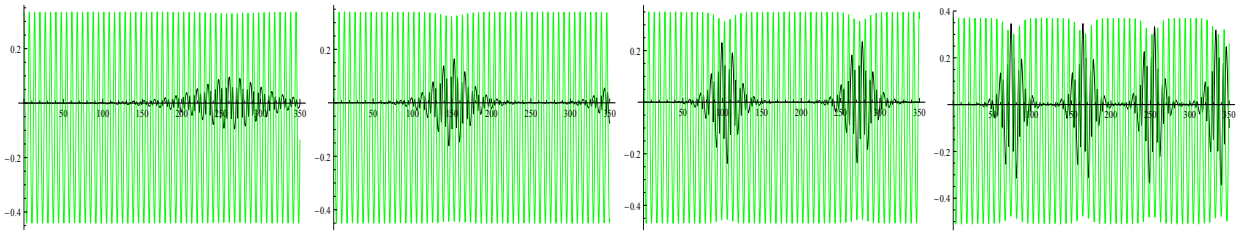

Figure 4: The solution $\theta = \theta(t)$ (black), $y = y(t)$ (green) to (12). From left to right, the values of y_0 are: $y_0 = 0.335$, $y_0 = 0.34$, $y_0 = 0.35$, $y_0 = 0.37$, corresponding to $\mathcal{E} \approx 0.0686$, $\mathcal{E} \approx 0.07$, $\mathcal{E} \approx 0.0755$, $\mathcal{E} \approx 0.0853$.

between oscillators, tiny torsional oscillations θ may suddenly increase their amplitude by taking some of the amplitude of vertical oscillations y. The quantity transferred seems to be an increasing function of y_0 and, therefore, of the total energy of the system (12). The starting time of the sudden increase seems to be a decreasing function of y_0. We tried other values of y_0: for $y_0 \leq 0.333$ one sees the appearance of torsional oscillations only if magnified by a factor 100, for $y_0 > 0.37$ the phenomenon becomes more and more accentuated. We conclude that

if the total energy is small then the oscillators are stable and merely transfer a negligible part of their own energy, whereas if the total energy is sufficiently large then tiny torsional oscillations may suddenly become, without intermediate stages, wider oscillations.

Hence, there seems to be no relation with the behavior of external forces, such as the wind. The only relevant parameter seems to be the energy, as suggested in [14, Section 5.6]. In order to confirm that only the amount of total energy $\mathcal{E}$ matters, we tried other couples of initial data satisfying (11) with $\dot{y}(0) \neq 0$. In all the cases considered, when $\mathcal{E} \leq 0.068$ we could display an increase of the θ-oscillations only after magnification by a factor 100, whereas when $\mathcal{E} \geq 0.0685$ there was a substantial energy transfer between the two oscillators. Let us characterize this phenomenon more in detail.

Take $\ell = 1$; if $\min\{y - \sin\theta, y + \sin\theta\} \geq -1/2$, then the total energy (7) may be written as

$$\mathcal{E} = \left(\frac{\dot{\theta}^2}{6} + \frac{\sin^2(\theta)}{2}\right) + \left(\frac{\dot{y}^2}{2} + \frac{y^2}{2} + \frac{y^3}{3}\right) + y\sin^2(\theta) =: \mathcal{E}^\theta(t) + \mathcal{E}^y(t) + \mathcal{E}^{\theta y}(t)$$

where $\mathcal{E}^\theta$ (resp. $\mathcal{E}^y$) denotes the (nonconstant!) energy of the oscillator θ (resp. y) while $\mathcal{E}^{\theta y}$ denotes the coupling energy. If $\min\{y - \sin\theta, y + \sin\theta\} < -1/2$, then the explicit form of $\mathcal{E}$ is slightly different but we maintain the same definition of $\mathcal{E}^\theta$ and $\mathcal{E}^y$ and we put all the "compensation terms" in the definition of $\mathcal{E}^{\theta y}$. Then, by neglecting $\mathcal{E}^{\theta y}$, in Figure 5 we plot the two energies $\mathcal{E}^\theta$ and $\mathcal{E}^y$ for the problem (12).

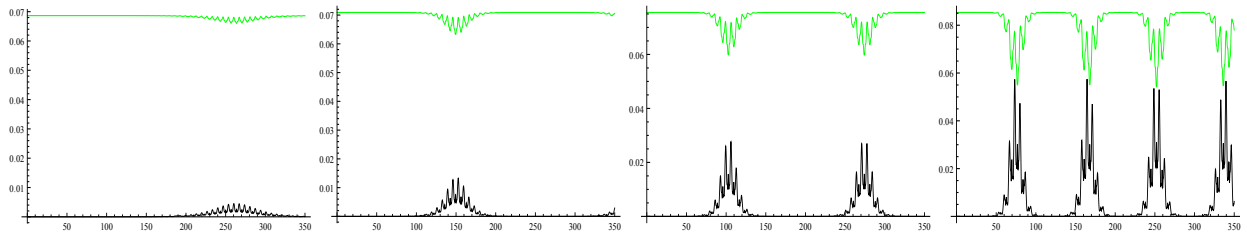

Figure 5: The energies $\mathcal{E}^\theta(t)$ (black) and $\mathcal{E}^y(t)$ (green) in (12). From left to right, the values of y_0 are: $y_0 = 0.335$, $y_0 = 0.34$, $y_0 = 0.35$, $y_0 = 0.37$.

It appears clearly that some of the energy of the y-oscillator suddenly transfers to the θ-oscillator.

2.2 Poincaré maps and the critical energy threshold

In order to compute the critical energy threshold, we study the solutions of system (5) from a different point of view. For simplicity, we take again $\ell = 1$ and (4) so that (8) reads

$$\begin{cases} \ddot{\theta} + 3\cos(\theta)\sin(\theta)(1 + 2y) = 0 \\ \ddot{y} + y + y^2 + \sin^2(\theta) = 0\,, \end{cases} \tag{13}$$

provided $\min\{y - \sin\theta, y + \sin\theta\} \geq -1/2$, which will always be the case for the experiments in this section. Since the energy (7) of the system

$$\mathcal{E}(\dot{\theta}, \dot{y}, \theta, y) := \frac{\dot{\theta}^2}{6} + \frac{\dot{y}^2}{2} + \frac{y^2}{2} + \frac{y^3}{3} + \frac{\sin^2(\theta)}{2} + y\sin^2(\theta)$$

is a constant of motion, for any $E_0 > 0$ the 3-dimensional submanifold $\mathcal{E}(\dot{\theta}, \dot{y}, \theta, y) = E_0$ of the phase space $\mathbb{R}^4$ is flow-invariant, that is, the motion is confined to this 3-dimensional energy surface. For geometrical reasons it is more practical to study a 2-dimensional section of this surface, the so-called *Poincaré section* [18, Section 11.5] whose construction adapted to the problem at hand we now give in detail.

First observe that also

$$\text{the plane } \theta = \dot\theta = 0 \text{ is flow-invariant} \tag{14}$$

and that equation (10) admits a periodic solution $\overline{y}(t)$ for all initial data $(y(0), \dot y(0)) = (0, y_1)$ with $y_1 \neq 0$ sufficiently small, in particular when $|y_1| \leq 1/\sqrt{6}$, see (22) below for an explanation of this bound. In such case, there exists a first $t_0 = t_0(y_1) > 0$ such that $\overline{y}(t_0) = 0$ and $\dot{\overline{y}}(t_0) = y_1$. Clearly, the pair $(\theta, y) = (0, \overline{y})$ is a periodic solution of system (13) with initial data $(\dot\theta(0), \dot y(0), \theta(0), y(0)) = (0, y_1, 0, 0)$.

Now fix $0 < E_0 \leq \frac{1}{12}$, see again (22) for the explanation of the upper bound, and let

$$\mathcal{U}_{E_0} := \left\{ (\theta_0, \theta_1) \in \mathbb{R}^2;\ \frac{\theta_1^2}{6} + \frac{\sin^2(\theta_0)}{2} < E_0 \right\}.$$

Moreover, for any $(\theta_0, \theta_1) \in \mathcal{U}_{E_0}$ we define

$$y_1 = y_1(E_0, \theta_0, \theta_1) := \sqrt{2E_0 - \sin^2(\theta_0) - \frac{\theta_1^2}{3}} > 0$$

so that $\mathcal{E}(\theta_1, y_1, \theta_0, 0) = E_0$ and $y_1 \in (0, 1/\sqrt{6}]$; then, by continuous dependence with respect to the initial data, it follows that there exists a first $T = T(\theta_0, \theta_1) > 0$ such that the solution of (13) with initial data

$$(\dot\theta(0), \dot y(0), \theta(0), y(0)) = (\theta_1, y_1(E_0, \theta_0, \theta_1), \theta_0, 0) \tag{15}$$

satisfies $y(T) = 0$ and $\dot y(T) > 0$. The Poincaré map $P_{E_0} : \mathcal{U}_{E_0} \to \mathbb{R}^2$ is then defined by

$$P_{E_0}(\theta_0, \theta_1) = (\theta(T), \dot\theta(T)) \tag{16}$$

where $(\theta(t), y(t))$ is the solution to (13)-(15). Note that, for such solution, one has $\mathcal{E} = E_0$. In view of (14), the origin $(0,0) \in \mathcal{U}_{E_0}$ is a fixed point for the map P_{E_0} for any $E_0 \in (0, 1/12]$; moreover, since the system (13) is conservative, the Jacobian $JP_{E_0}(0,0)$ of P_{E_0} at the origin has determinant equal to 1, so either both its eigenvalues have modulus 1, or they are both real. In the first case the origin is a stable fixed point for P_{E_0}, in the second case the origin is unstable. Hence, the simplest way to establish whether the system is in a stable or unstable state is to compute the eigenvalues of the Jacobian of the Poincaré map; this is done numerically.

Definition 1. (STABILITY)
Let $\lambda_1 = \lambda_1(E_0)$ and $\lambda_2 = \lambda_2(E_0)$ the complex eigenvalues of the Jacobian of the Poincaré map P_{E_0} at the origin $(0,0) \in \mathbb{R}^2$. Then $\lambda_1\lambda_2 = 1$ and two cases may occur:
(S) *if $|\lambda_1| = |\lambda_2| = 1$ and $\lambda_2 = \overline{\lambda_1}$ we say that (13) is torsionally stable;*
(U) *if $\lambda_1, \lambda_2 \in \mathbb{R}$ and $0 < |\lambda_1| < 1 < |\lambda_2|$ we say that (13) is torsionally unstable.*

The borderline situations where $\lambda_1 = \lambda_2 = 1$ or $\lambda_1 = \lambda_2 = -1$ are still in the stable regime, case (S). By continuous dependence, the transition to the unstable case may occur only in these situations and case (S) occurs at low energies E_0 whereas case (U) may occur only at higher energies. More precisely, we have seen in Section 2.1 that there exists $\overline{E} > 0$ such that the system (13) is stable (case (S)) whenever $0 < \mathcal{E} < \overline{E}$ whereas the system (13) is unstable (case (U)) whenever $\overline{E} < \mathcal{E} < \overline{E} + \delta$ for some $\delta > 0$.

Definition 2. (CRITICAL ENERGY THRESHOLD)
We call $\overline{E}$ the critical energy threshold of (13).

In order to understand the dynamics of the system and the importance the critical energy threshold we use the Poincaré maps. We now show that

the Poincaré maps explain the onset of instability, and therefore the critical energy threshold, with internal resonances.

In Figure 6 we represent some iterates of the map P_{E_0} with different initial data $(\theta(0), \dot\theta(0))$ close to $(0,0)$. The energies considered are $E_0 = 0.06,\ 0.067,\ 0.0685,\ 0.07$. Finer experiments show that the change of stability occurs for $E_0 \in (0.0679, 0.068)$ and hence the critical energy threshold satisfies

$$0.0679 < \overline{E} < 0.068\,.$$

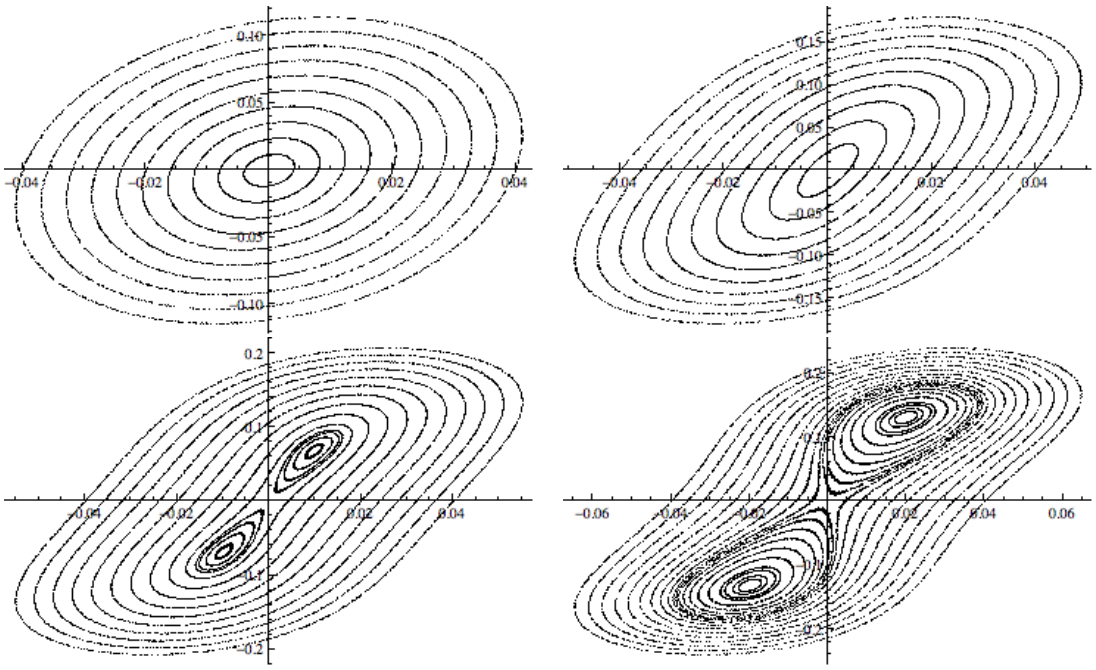

Figure 6: The Poincaré map for (13) for different values of the energy E_0: from left to right and top to bottom, the values of E_0 are 0.06, 0.067, 0.0685, 0.07.

The pictures in Figure 6 show that at low levels of energy, say $\mathcal{E} < \overline{E}$, any initial condition with small $(\theta(0), \dot\theta(0))$ leads to solutions with small $(\theta(t), \dot\theta(t))$ for all t, while at higher levels of energy, say $\mathcal{E} > \overline{E}$, any initial condition with small $(\theta(0), \dot\theta(0))$ leads to large values of $(\theta(t), \dot\theta(t))$ for some t. Figure 6 displays a period doubling bifurcation for the fixed points of the Poincaré map (16) parametrized by E_0. By (14) the origin is a fixed point of P_{E_0} for any value of E_0. When $E_0 < \overline{E}$, the critical energy threshold, the origin is stable. When $E_0 > \overline{E}$ the origin is unstable, and two stable periodic points branch out of the origin. A necessary condition for this bifurcation to take place is that the Jacobian of $P^2_{E_0} - I$ at $(0,0)$ ($P^2_{E_0}$ being the second iteration of the Poincaré map whereas I is the identity map) is not invertible, while the Jacobian of $P_{E_0} - I$ is invertible. Since $\det P_{E_0} = 1$, this implies that both eigenvalues of $JP_{E_0}(0,0)$ are equal to -1. This occurs at $E_0 = \overline{E}$. Then $P^2_{\overline{E}}(\theta_0, \theta_1) = (\theta_0, \theta_1) + o(\theta_0, \theta_1)$, so that small (θ_0, θ_1) correspond to solutions $\theta(t)$ close to a periodic solution whose period is half the period of $y(t)$. If $E_0 > \overline{E}$ two stable periodic points of period 2 appear: they represent periodic solutions $\theta(t)$ whose period is half the period of $y(t)$. Summarizing, the necessary condition for a period doubling bifurcation corresponds to a resonance between the oscillators; hence in absence of resonance the double oscillator is torsionally stable.

The period doubling bifurcation is caused by a resonance between the nonlinear oscillators and generates torsional instability.

This simple description is possible because we are dealing with a 2×2 model. Unfortunately, we will not have a so clear image of the phenomenon for the full bridge model, see Section 4.

3 Robustness of the single cross section model

We show here that the results obtained in Section 2 are robust. In particular, they are almost insensitive to a linearization with respect to θ, they qualitatively remain the same also in presence of more general forces, and the same phenomena remain visible under the effect of damping and forcing.

3.1 The effects of linearizing the angle

Since wide torsional oscillations should be expected, the angle θ may be far away from 0, but when this is the case, the bridge has already... collapsed! Therefore our analysis can be restricted to understanding under which conditions θ may become large. In this section we show that if we linearize (5) with respect to θ, then the results are qualitatively very similar, although the dependence of the system on the width 2ℓ is lost. We replace $\sin\theta \cong \theta$ and $\cos\theta \cong 1$, and set $x = \ell\theta$ to get

$$\begin{cases} \frac{\ddot{x}}{3} + \frac{\partial U(x,y)}{\partial x} = 0 \\ \ddot{y} + \frac{\partial U(x,y)}{\partial y} = 0\,. \end{cases} \tag{17}$$

The potential is now $U(x,y) = F(y+x) + F(y-x)$ and the energy is

$$\mathcal{E} = \frac{1}{2}\left(\frac{\dot{x}^2}{3} + \dot{y}^2\right) + U(x,y)\,.$$

By taking again (4), so that $F(s) = \frac{s^2}{4} + \frac{s^3}{6}$ when s is small, we obtain

$$U(x,y) = \frac{x^2}{2} + \frac{y^2}{2} + \frac{y^3}{3} + x^2 y \tag{18}$$

and system (17) becomes

$$\begin{cases} \ddot{x} + 3x + 6xy = 0 \\ \ddot{y} + y + y^2 + x^2 = 0\,. \end{cases} \tag{19}$$

In Figure 7 we display the Poincaré maps corresponding to (19) for energies $\mathcal{E} = 0.6$ and $\mathcal{E} = 0.7$.

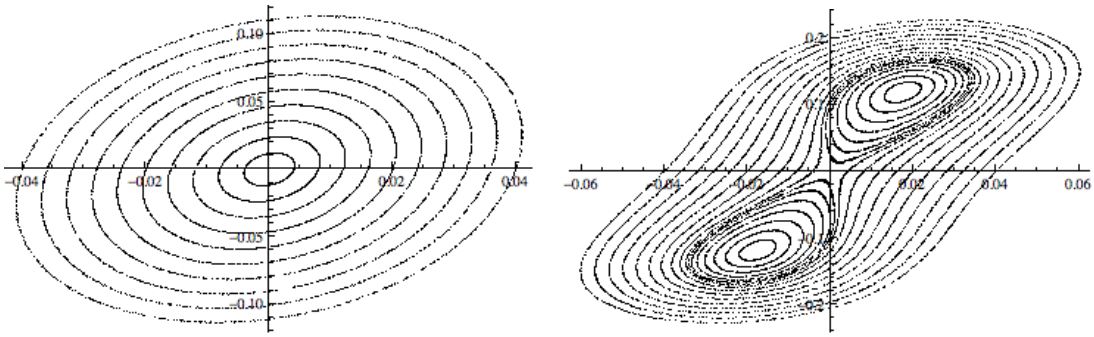

Figure 7: Poincaré maps after linearization with respect to θ.

It is quite clear that the linearization does not make any qualitative change to the pictures in Figure 6, but only a small quantitative change.

A further effect of the linearization of the angle is that (19) has a strong resemblance with the Henón-Heiles system which describes the motion of stars about the galactic center, see [21] and also [18, Section 11.6]. The Henón-Heiles system is

$$\begin{cases} \ddot{x} + x + 2xy = 0 \\ \ddot{y} + y - y^2 + x^2 = 0\,, \end{cases} \tag{20}$$

which, up to a factor $\frac{1}{3}$ on $\ddot{x}$, corresponds to (17) with

$$U(x,y) = \frac{x^2}{2} + \frac{y^2}{2} - \frac{y^3}{3} + x^2 y \, .$$

The origin $O \in \mathbb{R}^2$ lies in a crater of the graph of U whose depth equals the minimax level, also called the mountain-pass level, namely the least level of saddle points, which is $\frac{1}{6}$. The connected component containing the origin of the sublevel $U(x,y) \leq \frac{1}{6}$ is the equilateral triangle defined by

$$(x,y) \in \mathbb{R}^2, \qquad (2y+1)(y-\sqrt{3}x-1)(y+\sqrt{3}x-1) \leq 0 \, ,$$

see Figure 8. If the initial data $(x(0), y(0))$ lie inside the triangle and the (constant) energy $\mathcal{E}$ of (20) satisfies $\mathcal{E} \leq \frac{1}{6}$, then the solution to (20) is global in time and the orbit in the phase plane remains inside the triangle. On the other hand, solutions to (20) with $\mathcal{E} > \frac{1}{6}$ may blow up in finite time.

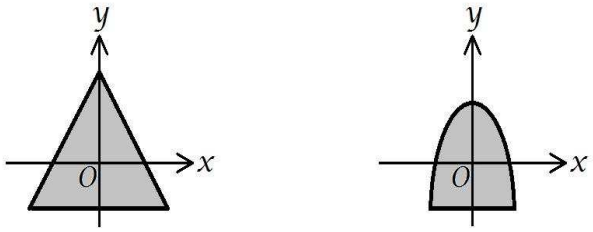

Figure 8: The regions of the phase plane where the solutions to (20) (left) and to (19) (right) are global.

On the other hand, the energy of (19) is given by

$$\mathcal{E} = \frac{\dot{x}^2}{6} + \frac{\dot{y}^2}{2} + \frac{x^2}{2} + \frac{y^2}{2} + x^2 y + \frac{y^3}{3} \, . \tag{21}$$

The potential part U of (21) is given by (18) and U has a strict local minimum at the origin O. The crater containing O has depth $\frac{1}{12}$ and the sublevel $U(x,y) \leq \frac{1}{12}$ is the half ellipse containing O and defined by

$$(x,y) \in \mathbb{R}^2, \qquad (2y+1)(6x^2+2y^2+2y-1) \leq 0 \, , \tag{22}$$

see Figure 8. If the initial data $(x(0), y(0))$ lie inside the half ellipse and the the total (constant) energy $\mathcal{E}$ in (21) satisfies $\mathcal{E} \leq \frac{1}{12}$, then the solution to (19) is global in time and the orbit in the phase plane remains inside the half ellipse. If $\mathcal{E} > \frac{1}{12}$ then the solution to (19) may blow up in finite time.

Remark 3. Up to a factor 3, (19) is integrable. Indeed, consider the system

$$\ddot{x} + x + 2xy = 0 \, , \qquad \ddot{y} + y + y^2 + x^2 = 0$$

and put $w(t) := y(t) - x(t)$ and $z(t) := y(t) + x(t)$. By adding and subtracting the equations, we obtain

$$\ddot{w} + w + w^2 = 0 \, , \qquad \ddot{z} + z + z^2 = 0$$

which is a decoupled system composed by two independent equations such as (10).

3.2 More general perturbations of linear forces

The purpose of this section is to confirm that the sudden appearance of oscillations in θ depends on nonlinear perturbations of Hooke's law applied to the hangers, no matter what such perturbation is. We consider again system (5) with potential (6) but with a more general F. More precisely, one may think to the function F

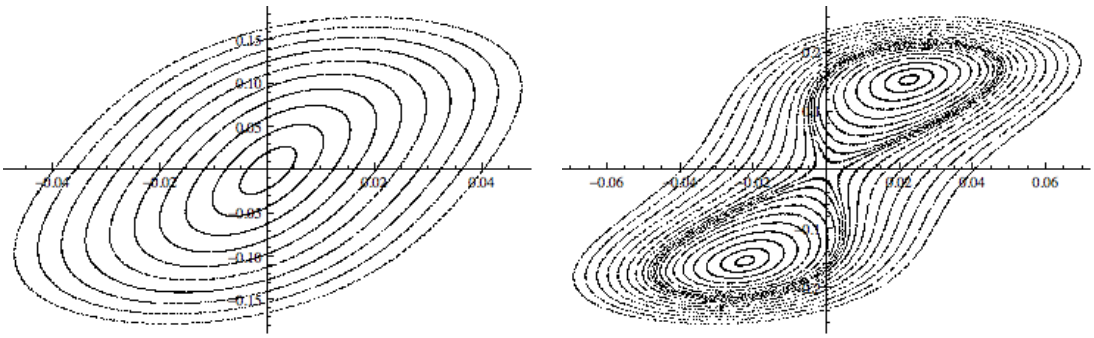

Figure 9: The Poincaré maps for different perturbations of linear forces.

as the truncated Taylor expansion of some arbitrary smooth function: $F(s) = c_2 s^2 + c_3 s^3 + c_4 s^4 + \dots$ Clearly, the constant part is irrelevant, while the linear part can be taken equal to zero by assuming that $(\theta, y) = (0, 0)$ is the equilibrium point where gravity balances the restoring force of the hangers; all the other terms of the expansion depend on the actual bridge. In Figure 9 we display the Poincaré map in the case $F(s) = \frac{s^2}{4} + \frac{s^3}{6} + \frac{s^4}{40}$ with $\mathcal{E} = 0.08$ and $\mathcal{E} = 0.085$. It is quite clear that the qualitative behavior of the system is the same as in the case of a purely cubic perturbation, see Figure 6.

This remark enables us to attempt an "at hand" description of how the appearance of torsional oscillations may occur. We have just seen that any kind of nonlinear restoring force $f = F'$ does not modify the qualitative behavior of the Poincaré map. We have seen in Section 3.1 that also the linearization with respect to θ does not modify the qualitative behavior of the Poincaré map. So, we may take $f(s) = \frac{1}{2}(s + s^3)$ and consider the system

$$\begin{cases} \ddot{x} + 3x(1 + x^2 + 3y^2) = 0 \\ \ddot{y} + y(1 + y^2 + 3x^2) = 0\,, \end{cases} \tag{23}$$

which should be seen as a simple prototype where some explicit computations give important information. We prove that the nonlinear frequency of x is larger than the frequency of y, which shows that the mutual position of x and y varies and may create the spark for energy transfer.

Proposition 4. *Let (x, y) be a nontrivial solution to (23). Let $\eta_1 < \eta_2$ be two consecutive critical points of $y(t)$. Then there exists $\xi \in (\eta_1, \eta_2)$ such that $x(\xi) = 0$.*

Proof. By using (23), one sees that

$$\frac{d}{dt}(\dot{x}\dot{y}^3) + 3\frac{d}{dt}\Big(xy(1 + x^2 + y^2)\Big)\dot{y}^2 = 0 \qquad \forall t \geq 0\,. \tag{24}$$

By integrating (24) by parts over (η_1, η_2) we obtain

$$\begin{aligned} 0 &= \int_{\eta_1}^{\eta_2} \frac{d}{dt}\Big(x(t)y(t)\,(1 + x(t)^2 + y(t)^2)\Big)\,\dot{y}(t)^2\,dt \\ &= -2\int_{\eta_1}^{\eta_2} x(t)y(t)\,(1 + x(t)^2 + y(t)^2)\,\dot{y}(t)\ddot{y}(t)\,dt \\ &= 2\int_{\eta_1}^{\eta_2} x(t)y(t)^2\,(1 + x(t)^2 + y(t)^2)\,(1 + y(t)^2 + 3x(t)^2)\dot{y}(t)\,dt \end{aligned}$$

where, in the last step, we used $(23)_2$. In the integrand, $y^2(1 + x^2 + y^2)(1 + y^2 + 3x^2) \geq 0$ and also $\dot{y}$ has fixed sign so that the integral may vanish only if $x(t)$ changes sign in (η_1, η_2). □

3.3 The effect of damping and forcing on the cross section

In this section we discuss some variants of the systems so far considered by adding damping and forcing terms. We believe that these variants are quite interesting in at least two respects. First, they show that the phenomena visible in the "stripped model" (without damping and forcing) persist in more detailed models. Second, they give rise to several natural questions such as the combination of damping/forcing terms, the sensitivity with respect to small perturbations, the relevance of the initial kinetic data $\dot\theta(0)$ and $\dot y(0)$; all these questions will be the target of future works.

Consider (13), where we already set $\ell = 1$, with the addition of a damping term in the y-equation:

$$\begin{cases} \ddot\theta + 3\cos(\theta)\sin(\theta)(1+2y) = 0 \\ \ddot y + \delta\dot y + y + y^2 + \sin^2(\theta) = 0\,, \end{cases} \tag{25}$$

where $\delta \geq 0$. We fix the initial conditions to be

$$10^4\,\theta(0) = y(0) = y_0\,, \qquad \dot\theta(0) = \dot y(0) = 0\,. \tag{26}$$

In Figure 10 we display the plots of the solution to (25)-(26) for two values of δ. These pictures should

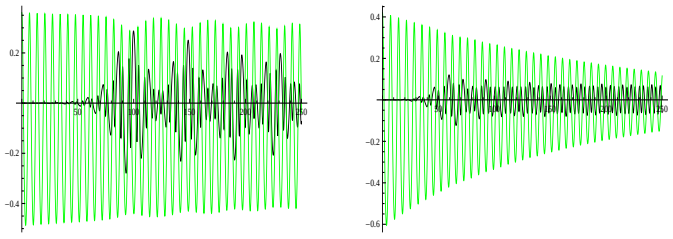

Figure 10: The solution $\theta = \theta(t)$ (black), $y = y(t)$ (green) to (25)-(26). The parameters are $y_0 = 0.36$ and $\delta = 0.001$ (left), $y_0 = 0.42$ and $\delta = 0.01$ (right).

also be compared with the undamped case, see Figure 4. It can be noticed that the energy transfer still occurs although more energy (that is, larger initial data) is needed to activate it. This is also what we saw in further experiments: the larger is δ, the larger needs to be y_0 in order to view energy transfer. And, of course, the amplitude of both the θ and y oscillations become small more quickly.

Slightly weaker appears the effect of a damping in the θ-equation; consider the system

$$\begin{cases} \ddot\theta + \delta\dot\theta + 3\cos(\theta)\sin(\theta)(1+2y) = 0 \\ \ddot y + y + y^2 + \sin^2(\theta) = 0\,, \end{cases} \tag{27}$$

where $\delta \geq 0$. With the same initial conditions (26), we obtained the plots displayed in Figure 11. Note that even for a "large" $\delta = 0.1$ (large if compared to the ones in Figure 10) the energy transfer is still visible without increasing y_0. However, for $0.1 < \delta < 0.15$, the amplitude of the θ-oscillation decreases considerably and almost disappears for $\delta > 0.15$.

Then we put some forcing term in both equations in order to insert energy into the structure; consider the system

$$\begin{cases} \ddot\theta + 3\cos(\theta)\sin(\theta)(1+2y) + \gamma\sin(t) = 0 \\ \ddot y + y + y^2 + \sin^2(\theta) + \gamma\sin(t) = 0\,, \end{cases} \tag{28}$$

where $\gamma \in \mathbb{R}$. From our experiments it seems that the sign of γ does not play a role while the amplitude $|\gamma|$ is more relevant. In Figure 12 we display the plots of the solutions to (28)-(26) for different values of γ.

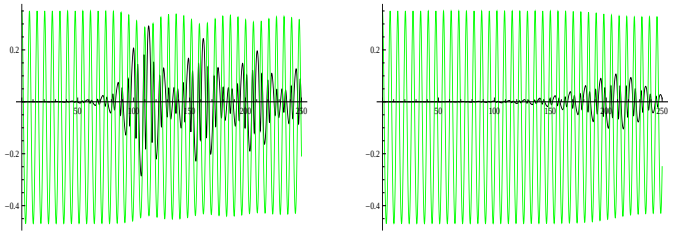

Figure 11: The solution $\theta = \theta(t)$ (black), $y = y(t)$ (green) to (27)-(26) with $y_0 = 0.35$. The damping parameters are $\delta = 0.01$ (left), $\delta = 0.1$ (right).

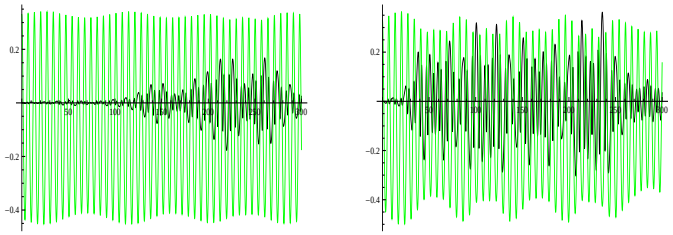

Figure 12: The solution $\theta = \theta(t)$ (black), $y = y(t)$ (green) to (28)-(26). The values are $\gamma = 0.002$ (left), $\gamma = 0.007$ (right).

We notice that the larger is $\gamma > 0$ the earlier is the starting instant of the torsional oscillation. Moreover, the amplitude of torsional oscillations θ is increasing with respect to γ while vertical oscillations y appear to be almost independent of γ. Figure 12 should also be compared with Figures 4, 10, and 11. Let us mention that completely similar behaviors were obtained for the damped/forced alternative systems (19) and (23).

4 The full bridge model: multiple cross sections

4.1 Description of the model

We model here the bridge by taking into account also its length: we use a discrete model with a number n of cross sections, see Figure 3. We label the cross sections by $i = 1, \dots, n$ and we assume that each cross section interacts with the two adjacent ones by means of attractive linear forces. We denote by y_i the downwards displacement of the midpoint of the i-th cross section and by θ_i the angle of deflection from horizontal of the i-th cross section. We assume that the mass of each beam modeling a cross section is $m = 1$ and its half-length is $\ell = 1$, independently of i. We have the following system of $2n$ equations:

$$\begin{cases} \frac{1}{3}\ddot{\theta}_i + U_{\theta_i}(\Theta, Y) = 0 \\ \ddot{y}_i + U_{y_i}(\Theta, Y) = 0 \end{cases} \qquad (i = 1, ..., n)\,, \tag{29}$$

where $(\Theta, Y) = (\theta_1 \dots, \theta_n, y_1, \dots, y_n) \in \mathbb{R}^{2n}$ and

$$U(\Theta, Y) = \sum_{i=1}^{n} \Big[F(y_i + \ell \sin\theta_i) + F(y_i - \ell \sin\theta_i) \Big] + \frac{1}{2} \sum_{i=0}^{n} \Big[K_y (y_i - y_{i+1})^2 + K_\theta (\theta_i - \theta_{i+1})^2 \Big]\,.$$

The choice of the nonlinear restoring force $f = F'$ is here more delicate. First of all, the hangers do not all behave similarly; according to [20, p.1624] *...the failure of long hangers is less critical than the failure of short hangers*, which implies that hangers and restoring forces depend on the longitudinal position. Also, the sustaining cable links all the hangers, so that they cannot be considered to behave independently from

each other. In a future work we will discuss these issues. Here, we choose a nonlinearity which appears reasonable and causes the same phenomenon that one observes in the single cross-section model; we take

$$f(s) = \frac{s + s^2 + s^3}{2} \quad \text{and then} \quad F(s) = \frac{s^2}{4} + \frac{s^3}{6} + \frac{s^4}{8}\,. \tag{30}$$

The constants $K_y, K_\theta > 0$ represent the vertical and torsional stiffness of the bridge; we choose $K_y = K_\theta = 10n$ because this value leads to realistic simulations. We set $y_0 = y_{n+1} = \theta_0 = \theta_{n+1} = 0$ to model the connection between the bridge and the ground. The total energy of the system

$$\mathcal{E}(\dot\Theta, \dot Y, \Theta, Y) = \frac{|\dot\Theta|^2}{6} + \frac{|\dot Y|^2}{2} + U(\Theta, Y) \tag{31}$$

is conserved. Let $\mathtt{dst} : \mathbb{R}^n \to \mathbb{R}^n$ be the discrete sine transform, that is the linear invertible map defined by

$$x_i = \frac{2}{n+1}\sum_{j=1}^{n} (\mathtt{dst}x)_j \sin\left(\frac{\pi ij}{n+1}\right) \qquad \text{and} \qquad (\mathtt{dst}x)_j = \sum_{i=1}^{n} x_i \sin\left(\frac{\pi ij}{n+1}\right)\,,$$

and note that, for any given mode $k \in \{1, \dots, n\}$ and $E_0 > 0$, there exists a unique $\alpha = \alpha(k, E_0) > 0$ such that $\mathcal{E}\left(0, \alpha(k, E_0)\mathtt{dst}(e_k), 0, 0\right) = E_0$, where e_k is the $k-$th element of the canonical basis of $\mathbb{R}^n$. We observe that if f were linear, then the initial condition $(0, \alpha(k, E_0)\mathtt{dst}(e_k), 0, 0)$ would raise a periodic solution to (29) for all k, E_0. If f is nonlinear, e.g. as in (30), by a minimization algorithm we can compute numerically $Y_0(k, E_0), Y_1(k, E_0) \in \mathbb{R}^n$ such that $|Y_0(k, E_0)|$ and $|Y_1(k, E_0) - \alpha(k, E_0)\mathtt{dst}(e_k)|$ are small and $(0, Y_1(k, E_0), 0, Y_0(k, E_0))$ lies on the orbit of a periodic solution to the nonlinear problem (29). Let $T = T(k, E_0) > 0$ be the period and let $\Psi_T : \mathbb{R}^{2n} \to \mathbb{R}^{2n}$ be defined by

$$\Psi_T(\Theta_1, \Theta_0) = \Big(\dot\Theta(T), \Theta(T)\Big)\,, \tag{32}$$

where $(\Theta(t), Y(t))$ is the solution to (29) with initial conditions

$$\Big(\dot\Theta(0), \dot Y(0), \Theta(0), Y(0)\Big) = (\Theta_1, Y_1(k, E_0), \Theta_0, Y_0(k, E_0))\,. \tag{33}$$

We study the Jacobian $J\Psi_T(0,0)$ of Ψ_T computed at $(\Theta_1, \Theta_0) = (0, 0)$. In order to compute the derivatives of this map, we consider a variation $\Xi = (\xi_1 \dots, \xi_n)$ of $\Theta \equiv 0$ and we integrate the equations

$$\frac{1}{3}\ddot\xi_i + \sum_{j=1}^{n} U_{\theta_i\theta_j}(0, Y)\xi_j = 0 \qquad\qquad (i = 1, ..., n)\,;$$

the l-th column of $J\Psi_T(0,0)$ equals the solution $(\dot\Xi(T), \Xi(T))$ at time T of such problem with initial conditions $(\dot\Xi(0), \Xi(0)) = \eta_l$ $(l = 1, ..., 2n)$, where η_l is the l-th element of the canonical basis of $\mathbb{R}^{2n}$. We remark that the so obtained matrix is related to, but it *is not* the Jacobian of a Poincaré map.

4.2 Dynamics of the n-beam system

Our first result is that **the n-beam system behaves essentially as the single beam system.** In particular, all numerical evidence points to the existence of a critical energy threshold $\overline{E}$; when the energy of the system is smaller than $\overline{E}$ the bridge is stable, while when the energy of the system is larger than $\overline{E}$ the bridge is unstable, that is a very small perturbation in any θ_i-variable can lead to a significant torsional motion due to a substantial energy transfer between oscillators. Such threshold depends on the number of cross sections n and the on the mode k. We experimented with various values of n, but we display here only the results with $n = 16$, which seem to provide a good description of the system without cluttering the pictures. Figures 13, 14, 15, 16 represent the solutions to the system (29) with initial conditions (33) and

$$(k, E_0) = (1, 500), (2, 1000), (3, 3000), (4, 3000)\,.$$

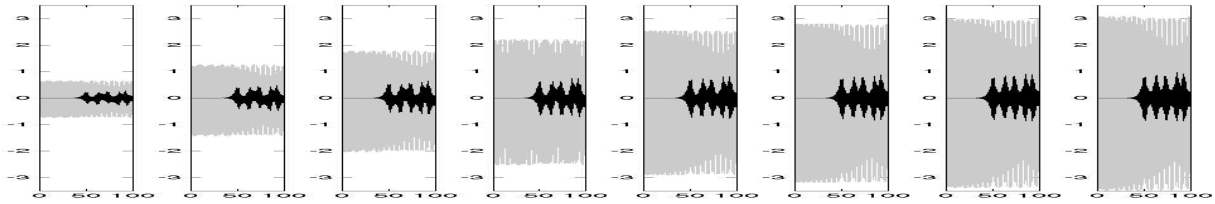

Figure 13: Unstable torsional oscillations (black) and vertical oscillations (grey) of the cross sections of the bridge, with $(k, E_0) = (1, 500)$. Movie at `http://mox.polimi.it/~gianni/bridge1.mp4`

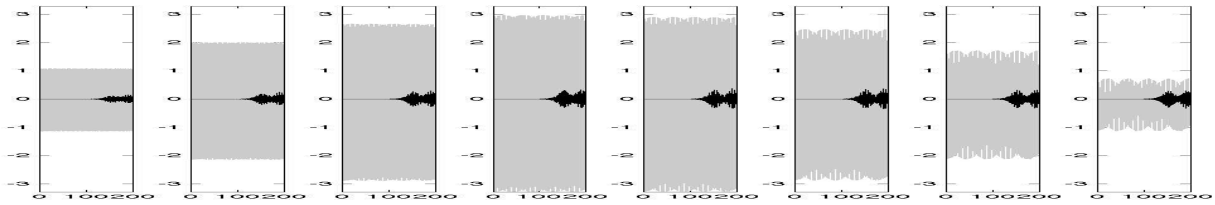

Figure 14: Unstable torsional oscillations (black) and vertical oscillations (grey) of the cross sections of the bridge, with $(k, E_0) = (2, 1000)$. Movie at `http://mox.polimi.it/~gianni/bridge2.mp4`

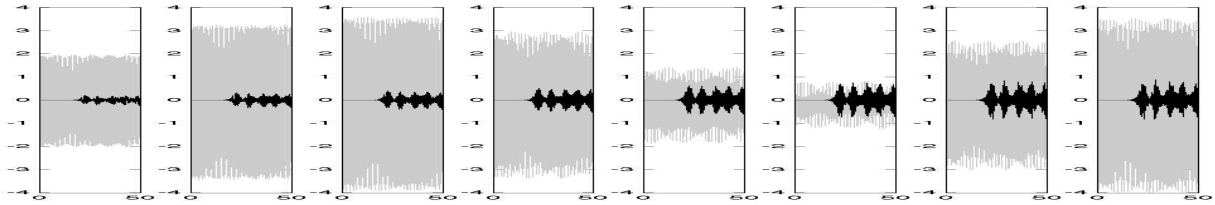

Figure 15: Unstable torsional oscillations (black) and vertical oscillations (grey) of the cross sections of the bridge, with $(k, E_0) = (3, 3000)$. Movie at `http://mox.polimi.it/~gianni/bridge3.mp4`

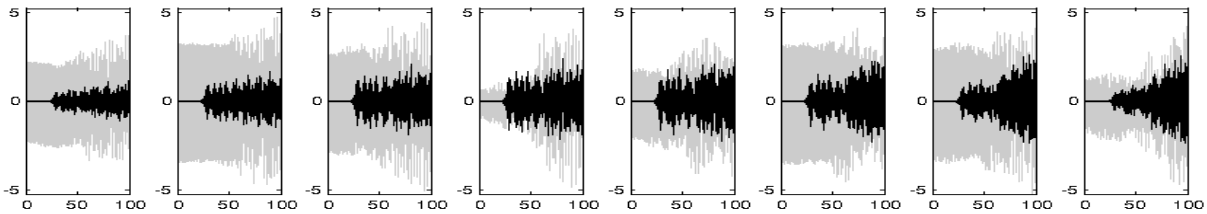

Figure 16: Unstable torsional oscillations (black) and vertical oscillations (grey) of the cross sections of the bridge, with $(k, E_0) = (4, 4000)$. Movie at `http://mox.polimi.it/~gianni/bridge4.mp4`

In all the pictures the first line represents $\theta_i(t)$ and the second line represents $y_i(t)$, $i = 1, \dots, 8$. We only display (θ_i, y_i) for $i = 1 \dots, 8$ because $(\theta_i, y_i) \approx (\theta_{17-i}, y_{17-i})$ if k is odd and $(\theta_i, y_i) \approx -(\theta_{17-i}, y_{17-i})$ if k is even. A different point of view of the results of our experiments is provided by the movies available at the links in the captions of the figures. There one can see the actual dynamics of the discretized bridge, and in particular the similarity to the original movie of the Tacoma Narrows Bridge collapse [44]. We observe that the motion of the angular coordinates is negligible at first, but after a while it becomes significant. Clearly, if this were a real bridge, it would collapse.

Next, we consider the damped version of (29), that is

$$\begin{cases} \frac{1}{3}\ddot{\theta}_i + U_{\theta_i}(\Theta, Y) + \delta\dot{\theta}_i = 0 \\ \ddot{y}_i + U_{y_i}(\Theta, Y) + \delta\dot{y}_i = 0 \end{cases} \qquad (i = 1, ..., 16)\,, \tag{34}$$

where $\delta > 0$ is a damping parameter. The experiments show that the weakly damped bridge behaves as the undamped bridge, that is we still observe an energy threshold above which the torsional motion is unstable, provided δ is sufficiently small. A large value of the damping parameter dissipates the energy very rapidly, and then the instability is prevented. Figure 17 represents the solution to system (34), with $(k, E_0) = (1, 1000)$ and $\delta = 0.01$.

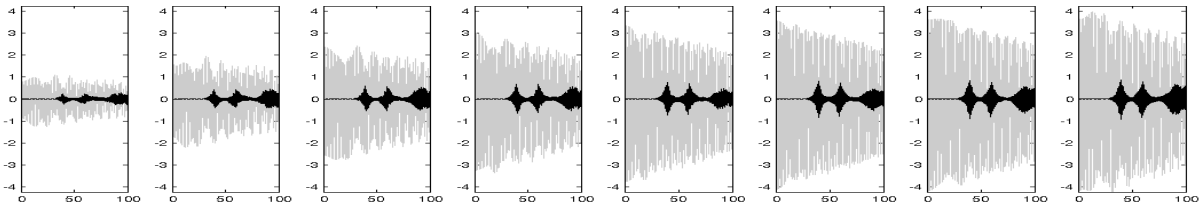

Figure 17: Unstable torsional oscillations (black) and vertical oscillations (grey) of the cross sections of the bridge, with $(k, E_0) = (1, 1000)$ and damping $\delta = 0.01$.

Remark 5. We also followed a less rigorous but simpler procedure, inspired to the experiments for the single cross section, see (12). Take again (30) and $n = 16$; consider (29) with initial data

$$\dot{\Theta}(0) = \dot{Y}(0) = 0\,, \quad 10^4\theta_i(0) = y_i(0) = \overline{y}\sin\left(\frac{ik\,\pi}{17}\right) \quad (i = 1, ..., 16)$$

where k denotes the mode we wish to perturb and $\overline{y} \neq 0$ serves as a measure of the energy $\mathcal{E}$. We have found that if $|\overline{y}|$ is small then torsional oscillations remain small, whereas if $|\overline{y}|$ is sufficiently large then there is a sudden transfer of oscillations from the y_i to the θ_i. The value where this transition occurs strongly depends on the mode k. This procedure, which is much simpler than the one described above, does not allow to give a precise definition of the critical energy threshold nor an exact procedure how to determine it.

4.3 Stability of the n-beam system

Our second result is that **the stability of the system can be evaluated by computing the eigenvalues of** $J\Psi_T(0, 0)$. We observed that the fatal instability may take a long time to manifest itself, therefore one may not trust the numerical integration of the system, unless such integration has been performed for a rather long time and with a sufficient degree of accuracy. But it turns out that there is a shortcut. In principle, when $n > 1$ one cannot infer the full stability of the system from its linear stability, that is having all eigenvalues of $J\Psi_T(0, 0)$ of modulus 1. On the other hand, we have numerical evidence that the model is torsionally stable if and only if all the eigenvalues of $J\Psi_T(0, 0)$ lie on the unit circle (in the conservative case) or inside the unit circle (in the damped case). In the graphs in Figure 18 we display the largest modulus of the

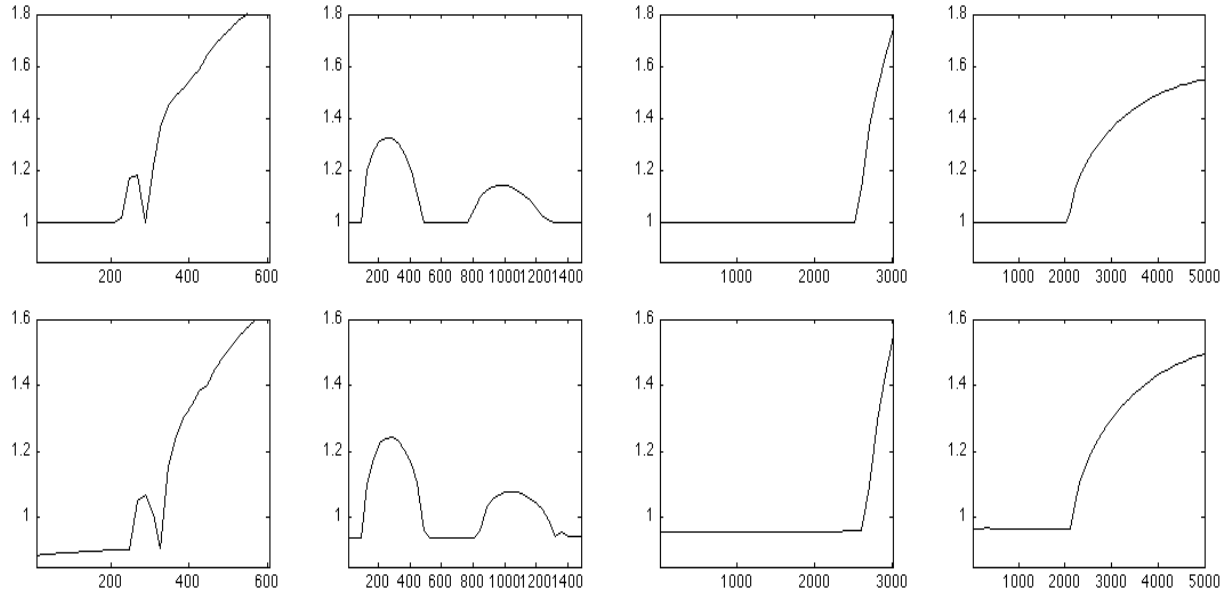

Figure 18: Largest modulus of the eigenvalues of $J\Psi_T(0,0)$ versus energy, $k = 1, 2, 3, 4$. Conservative case (first line), damped case (second line).

eigenvalues of $J\Psi_T(0,0)$ as a function of the energy E_0, with $k = 1, 2, 3, 4$. The first line is the conservative case, while the second line is the damped case with $\delta = 0.01$.

It appears that for all k there exists a largest $\overline{E}_k > 0$ such that the k-th mode is stable whenever $\mathcal{E} < \overline{E}_k$. Figure 18 shows that $\overline{E}_k$ depends on k and the effective critical energy threshold satisfies

$$\overline{E} \leq \min_{1 \leq k \leq n} \overline{E}_k \,.$$

The pictures also clearly display that the system is stable (in the conservative case) or asymptotically stable (in the damped case) when the energy is below a threshold, while it becomes unstable above such threshold. It turns out that, for higher levels of energy, the system may become stable again, but this has a purely theoretical (mathematical) relevance, since in order to ensure that the bridge is safe, one should consider only the lower energy threshold. All our experiments have shown that the system is stable, that is the torsional oscillations remain negligible, whenever it is linearly stable.

4.4 Our explanation of the Tacoma collapse

The starting point of our analysis is the system (2) introduced by McKenna [26] which describes the oscillations of a cross section of a suspension bridge by means of a system of coupled nonlinear oscillators. We first isolate the system by neglecting internal friction and external forces. Then, by choosing an *arbitrary* nonlinear force f due to the hangers, we show that there can be a sudden transfer of energy between the two oscillators, see Section 2.1. This occurs only at certain energy levels and the Poincaré maps give an effective way to determine the energy threshold where this transfer may occur, see Section 2.2. These results are robust and remain visible under fairly different variants of the model, see Section 3. We then model the entire bridge with a finite number of cross sections interacting with the adjacent ones, see Section 4. We show that the Poincaré type maps can be used to compute the critical energy threshold which, if exceeded, leads to the possibility of a switch between vertical and torsional oscillations. Our results allow to conclude that the only important parameter to be computed is precisely the critical energy threshold and it does not matter how this threshold is reached. So, any kind of external action inserting energy inside the structure may overcome the critical threshold of the bridge and give rise to uncontrolled oscillations. The critical

energy threshold is a parameter intrinsic of the bridge and depending only on its structural parameters such as width, length, rigidity, mass, elasticity, stiffness, and distance between hangers.

In Section 5.2 we describe the collapses of the Broughton Suspension Bridge and of the Angers Bridge, which were caused by a *light and precise* external solicitation that gave rise to resonance with the natural frequencies of the bridges. This has nothing to do with the *violent and disordered* solicitation of the wind at the TNB. By no means, one may expect that a random and variable wind might match *exactly* the natural frequency of a bridge.

The model we suggest here views the bridge as an elastic structure formed by many coupled nonlinear oscillators whose frequencies may create internal resonances. Nonlinearity yields frequencies that vary with the energy involved and, therefore, resonances may occur only if enough energy is inserted into the structure.

We believe that the TNB has collapsed because, on November 7, 1940, the wind inserted enough energy to overcome the critical energy threshold which gave rise to internal resonances that were the onset of torsional oscillations. No matter of what was its angle of attack or its frequency, the only important feature of the wind was the amount of energy it inserted into the bridge. Future bridges should be planned with structural parameters yielding very large critical energy thresholds.

5 Appendix: Prior explanations to the Tacoma Narrows Bridge collapse

5.1 Structural failure

The first natural explanation of the collapse is a mistake in the project. From the New York Times [32, p.5] we quote a comment by C.A. Andrew, chief engineer in charge of constructing the bridge, who claims that *...the collapse probably was due to the fact that flat, solid girders were used along one side of the span. These girders, he said, caught the wind like a kite and caused the bridge to sway*. However, this explanation appears too simplistic and the video of the collapse does not show the TNB as a kite! Moreover, as we have seen in Section 1.1, Moisseiff was not considered responsible for the collapse. Therefore, although some mistake was certainly present in the project (otherwise the original TNB would still stand!), these mistakes were certainly not so trivial.

Several people attempted to justify the collapse with a structural failure, as if some components might have reacted too weakly to the strong wind. Delatte [10, p.31] suggests that *A contributing factor may have been slippage of a band that retained the cables*. Then, by invoking [13, p.226], he writes that *...on November 7 a cable band slipped out of place at mid-span, and the motions became asymmetrical, like an airplane banking in different directions. The twisting caused metal fatigue, and the hangers broke like paper clips that had been bent too often*. This colorful description was not confirmed by subsequent studies.

According to [10, p.30], one of the conclusions of the Report [1] was that *The failure of the cable band on the north end, which was connected to the center ties, probably started the twisting motion of the bridge. The twisting motion caused high stresses throughout the bridge, which led to the failure of the suspenders and the collapse of the main span*. This kind of "domino effect" was not analyzed further in the sequel and, a few years after the collapse, Steinman [42] wrote that the ties *...permitted - not caused - the catastrophic oscillations that wrecked the structure*.

The engineer D.B. Steinman designed two pioneering suspension bridges, the Thousand Islands Bridge (1938) and the Deer Isle Bridge (1939), which had similar narrow and flexible structures as the TNB, see Figure 19. As mentioned by [10, p.33], *Both bridges exhibited substantial oscillations in the wind and required stiffening with cable ties. Vertical and torsional motions were both observed. The cables ties substantially reduced, but did not eliminate, the motions, and were thought to be an adequate repair*. This means that the phenomenon observed in the TNB is present in similar bridges and, therefore, the collapse cannot be attributed to a structural failure.

Steinman [41] claimed that the Report [1] *...leaves many questions unanswered. It does not tell what combinations of cross-sections produce aerodynamic instability, how aerodynamic instability can be reasonably predicted or readily tested, nor how it can be prevented*. His final observation is that *It is more scientific to*

Figure 19: The Thousand Islands Bridge (left) and the Deer Isle Bridge (right).

eliminate the cause than to build up the structure to resist the effect. This means that the answer to **(Q)** has to be sought **inside the bridge**.

5.2 Resonance

In an article appeared in the New York Times [33] a couple of days after the collapse, one may read *Like all suspension bridges, that at Tacoma both heaved and swayed with a high wind. It takes only a tap to start a pendulum swinging. Time successive taps correctly and soon the pendulum swings with its maximum amplitude. So with the bridge. What physicists call resonance was established, with the result that the swaying and heaving exceeded the limits of safety.*

According to [10, p.31], the Federal Report [1] concluded that *...because of the TNB's extreme flexibility, narrowness, and lightness, the random force of the wind that day caused the torsional oscillations that destroyed the bridge. The Authors believed that wind-induced oscillations approached the natural frequencies of the structure, causing resonance (the process by which the frequency of an object matches its natural frequency, causing a dramatic increase in amplitude).*

Most people believe that this explanation overlooks the important question as to how wind, random in nature, could produce a precise periodic impulse. For instance, the mathematicians Lazer-McKenna [25, Section 1] point out that *...the phenomenon of linear resonance is very precise. Could it really be that such precise conditions existed in the middle of the Tacoma Narrows, in an extremely powerful storm*? Also the physicists Green-Unruh [19] mention that *...making the comparison to a forced harmonic oscillator requires that the wind generates a periodic force tuned to the natural frequency of the bridge*. Among engineers, Scanlan [37] discards the possibility of resonance by writing *Others have added to the confusion. A recent mathematics text, for example, seeking an application for a developed theory of parametric resonance, attempts to explain the Tacoma Narrows failure through this phenomenon*. Moreover, Billah-Scanlan [6] make a fool of physics textbooks who attempt to explain the TNB collapse with resonance.

We agree with all these criticisms. Probably, the reason why the Tacoma collapse was attributed to resonance is hidden in history. The Broughton Suspension Bridge was built in 1826 and collapsed in 1831 due to mechanical resonance induced by troops marching over the bridge in step. A bolt in one of the stay-chains snapped, causing the bridge to collapse at one end, throwing about 40 men into the river. As a consequence of the incident, the British Army issued an order that troops should "break step" when crossing a bridge. The Angers Bridge was a suspension bridge over the Maine River in France. It was built between 1836 and 1839 and collapsed on April 16, 1850, while a battalion of French soldiers was marching across it, killing 226 of them. The battalion arrived during a powerful thunderstorm when the wind was making the bridge oscillate. When the soldiers began to cross, they gave the wind still more purchase. As usual in crossing that bridge, the soldiers had been ordered to break step and to space themselves farther apart than normal. However, their efforts to match the swaying and keep their balance has caused them to involuntarily march with the same cadence, contributing to the resonance. So, the failure was attributed to a combination of dynamic load due to the storm and the soldiers, particularly as they seem to have been somewhat in step.

This behavior is similar to what has been more recently observed on the London Millennium Bridge where the bridge started to sway from side to side and pedestrians fell spontaneously into step with the vibrations, thereby amplifying them, see [36]. Clearly, these accidents have nothing to do with what happened at the TNB. In Broughton and Angers the external forcing was an extremely precise periodic solicitation which was probably similar to one of the eigenfunctions of the vibrating plate sustaining the bridges.

Summarizing, mechanical resonance, intended as a perfect matching between the exterior wind and the parameters of the bridge, is not the culprit for the TNB. But, maybe, some kind of resonance may be found **inside the bridge**.

5.3 Vortices

Every oscillating structure has its own natural frequencies and resonance occurs if the excitation force acts periodically and with one of the natural frequencies. Due to the non-streamlined shape of the bridge, a possible candidate of the periodicity in the wind force was the so-called vortex shedding. These wakes are accompanied by alternating low-pressure vortices on the downwind side of the body, the so-called von Kármán vortex street. As a consequence, the bridge would move towards the low-pressure zone, in an oscillating movement called vortex-induced vibration. If the frequency of vortex shedding matches the natural frequency of the bridge, then the structure will begin to resonate and oscillations may become self-sustaining.

Von Kármán proposed that the motion seen on the day of the collapse was due to these vortices and that the von Kármán street wake reinforced the already present oscillations and caused the center span to violent twist until the bridge collapse, see [10, p.31]. But, according to Scanlan [37, p.841], *...some of the writings of von Kármán leave a trail of confusion ... it can clearly be shown that the rhythm of the failure (torsion) mode has nothing to do with the natural rhythm of shed vortices following the Kármán vortex street pattern*. And, indeed, the calculated frequency of a vortex caused by a 68 km/h wind is 1 Hz, whereas the frequency of the torsional oscillations measured by Farquharson was 0.2 Hz, see [6, p.120]. The conclusion in [6, p.122] is that *...we see the flutter vortex trail as a consequence, not as a primary cause*. Also Green-Unruh [19, Section III] claim that *...the von Kármán vortex street forms at a frequency determined by the geometry and the wind velocity. These vortices form independently of the motion and are not responsible for the catastrophic oscillations of the TNB*. Their own conclusion is similar, namely *...vortices are also produced as a result of the body's motion*.

In his autobiography [46, p.4], von Kármán gave his opinion about men of science in the 20th century, see also [24, Footnote 2, p.538]: *Einstein was the greatest ... he had four great ideas. Most other great names had one or, at most, two. I had ... three and a half*. It is clear that with such an attitude, von Kármán attracted several unpleasant comments among scientists. For instance, while discussing his theory of thin plates, Truesdell [45, pp.601-602] writes *...the von Kármán theory has always made me feel a little nauseated as well as very slow and stupid...* After some objections, Truesdell concludes that *...these objections do not prove that anything is wrong with von Kármán strange theory. They merely suggest that it would be difficult to prove that there is anything right about it*.

A doubt is legitimate: are von Kármán vortices discarded just because... they are due to von Kármán himself? Von Kármán died in 1963 and, probably, since then the number of his enemies decreased. Only much later, in 2000, the vortex theory was partially readmitted by Larsen who writes [23, p.247] *...the vortex street may cause limited torsion oscillations, but cannot be held responsible for divergent large-amplitude torsion oscillations*. And indeed, what remained obscure until that time was a deep understanding of how vortices may be responsible for the wind-excited twisting motion. Larsen [23, p.245] claims that *The key to the torsion instability mechanism is the formation and drift of large-scale vortices on the cross section. A discrete vortex simulation of the flow around a simplified model of the Tacoma Narrows section shape, in which the angle of attack changes stepwise from* 0 *to* 10°*, highlights the vortex dynamics involved*. Roughly speaking, it is claimed that the variation of the angle of attack creates an alternation of vortices characterized by the direction of rotation and the position above/below the roadway. These vortices are

also due to the H-form of the cross section and may either push up or pull down the endpoints of the cross section. The variation of the angles also generates extra energy that gives rise to higher amplitudes of torsional oscillations and the cross section oscillates in a self-sustaining motion. Design modifications, such as replacing the H-shaped section of the deck with an open girder, that would have rendered the original TNB more aerodynamically stable are also suggested by Larsen. This explanation seems to have convinced the engineering community since [23] received the "Outstanding Paper Award" remitted each year to the author of a paper published in the issues of the IABSE Journal Structural Engineering International.

Although this theory may describe the self-exciting phenomenon and the increase of the width of torsional oscillations, it fails to answer the fundamental question **(Q)**, it does not explain how the torsional oscillation starts. An explanation with stepwise angles of attack would imply that the wind did not vary the angle of attack for a long time and, suddenly, without any intermediate stage, it started varying the angle of attack creating a torsional motion. We also fail to understand the relevance of the experiments in [23]: it appears somehow obvious to us that if the wind is known to vary stepwise the angle of attack of about 10°, then the movement of the cross section of the roadway will be quite similar to a swing. But did the wind really vary stepwise the angle of attack on November 7, 1940? Recall that resonance is discarded precisely because nobody believes in "regular" winds... Skeptic comments on the Larsen work were also made by Green-Unruh [19] who write *...despite this success, this analysis is somewhat incomplete given the data available* and claim that *...the Larsen model does not adequately explain data at around 23 m/s*, which was the wind velocity the day of the TNB collapse.

Green-Unruh try to pursue the explanation suggested by Larsen under three different aspects: they study how vortices drift near boundaries, how a vortex drifts near the trailing edge of the bridge, and the production of vortices at the leading edge. The conclusion in [19] contains several criticisms on their own work; they write *The detailed method through which the oscillatory behavior is established may require further details ... the range of wind speeds where the model is applicable has not been fully established. At the extreme high and low values, computational calculations become less reliable...* In our opinion, this is what happens for general phenomena: as long as the phenomenon is in a suitable range, any explanation is satisfactory. But the TNB collapse did not occur in a "normal" situation and hence, instead of attributing to the wind all the responsibility of the TNB collapse, one should investigate deeper what happens **inside the bridge**.

5.4 Flutter theory

Flutter is a self-feeding and potentially destructive vibration where aerodynamic forces on an object couple with a structure's natural mode of vibration to produce rapid periodic motion. Flutter may occur in any object within a strong fluid flow, under the conditions that a positive feedback occurs between the structure's natural vibration and the aerodynamic forces. That is, the vibrational movement of the object increases an aerodynamic load, which in turn drives the object to move further. If the energy input by the aerodynamic excitation in a cycle is larger than that dissipated by the damping in the system, the amplitude of vibration will increase, resulting in self-exciting oscillations.

While discussing oscillations in bridges, the physicist Rocard [35, p.185] attributes to Bleich [7] *...to have pointed out the connection with the flutter speed of aircraft wings... He distinguishes clearly between flutter and the effect of the staggered vortices and expresses the opinion that two degrees of freedom (bending and torsion) at least are necessary for oscillations of this kind.* In [8, pp.246-247] it is assumed that the bridge is subject to a natural steady state oscillating motion and the flutter speed is defined as follows. *With increasing wind speed the external force necessary to maintain the motion at first increases and then decreases until a point is reached where the air forces alone sustain a constant amplitude of the oscillation. The corresponding velocity is called the critical velocity or flutter speed.* The importance of the flutter speed is then described by noticing that *...below the critical velocity V_c an exciting force is necessary to maintain a steady-state motion; above the critical velocity the direction of the force must be reversed (damping force) to maintain the steady state motion. In absence of such a damping force the slightest increase of the velocity above V_c causes augmentation of the amplitude.* This means that, if exceeded, the flutter speed, which is

seen as a critical input of external energy in [14], may give rise to uncontrolled phenomena such as torsional oscillations. Rocard [35, p.101] claims that the fundamental contribution of his own work is a *...precise method of calculating the critical speed of wind for any given suspension bridge*. He uses the parameters of the TNB and concludes that his computations lead to a critical speed of wind basically coinciding with the speed of the wind the day of the collapse, see [35, p.158].

Further credit to [7] is given in [39, p.80] where one can read *...Bleich's work ... ultimately opened up a whole new field of study. Wind tunnel tests on thin plates suggested that higher wind velocities increased the frequency of vertical oscillation while decreasing that of torsional oscillation*. However, the conclusion is that *...Bleich's work could not be used to explain the Tacoma Narrows Bridge collapse*. And, as far as we are aware, Rocard's method to determine the flutter speed was not used in later projects.

While referring explicitly to the work by Bleich and Rocard, Billah-Scanlan [6, p.122] write that *Another error accompanying many accounts has been the confusion of the phenomenon of bridge flutter with that of airplane wing flutter as though they were identical*. Billah-Scanlan also emphasize that *...forced resonance and self-excitation are fundamentally different phenomena* and they claim that their work demonstrates that *...the ultimate failure of the bridge was in fact related to an aerodynamically induced condition of self-excitation or "negative damping" in a torsional degree of freedom*. The negative damping together with the torsional degree of freedom caused the torsional flutter so that, as the roadway rotated, the wind force acting on the surface changed, when the bridge rotated back the forces pushed the bridge in the opposite direction. They claim that this negative damping effect and increase in rotation lead up to the torsional oscillation that caused the collapse of the bridge.

Larsen [23, p.244] writes that *...Billah and Scanlan ... fail to connect the vortex pattern to the shift of apparent section damping from positive to negative, which signifies the onset of torsional instability*. Our own opinion is that self-excited oscillations may appear only if some oscillations already exist, but what created the "first" torsional oscillation? So, also this explanation fails to answer to **(Q)** and the answer is presumably hidden somewhere **inside the bridge**.

Acknowledgement. The authors are grateful to Antonio Giorgilli (Università degli Studi di Milano) for useful discussions and suggestions.

References

[1] O.H. Ammann, T. von Kármán, G.B. Woodruff, *The failure of the Tacoma Narrows Bridge*, Federal Works Agency (1941)

[2] G. Arioli, F. Gazzola, *Existence and numerical approximation of periodic motions of an infinite lattice of particles*, Zeit. Angew. Math. Phys. **46**, 898-912 (1995)

[3] G. Arioli, F. Gazzola, *Periodic motions of an infinite lattice of particles with nearest neighbor interaction*, Nonlin. Anal. TMA **26**, 1103-1114 (1996)

[4] G. Arioli, F. Gazzola, S. Terracini, *Multibump periodic motions of an infinite lattice of particles*, Math. Z. **223**, 627-642 (1996)

[5] E. Berchio, A. Ferrero, F. Gazzola, P. Karageorgis, *Qualitative behavior of global solutions to some nonlinear fourth order differential equations*, J. Diff. Eq. **251**, 2696-2727 (2011)

[6] K.Y. Billah, R.H. Scanlan, *Resonance, Tacoma Narrows bridge failure, and undergraduate physics textbooks*, Amer. J. Physics **59**, 118-124 (1991)

[7] F. Bleich, *Dynamic instability of truss-stiffened suspension bridges under wind action*, Proceedings ASCE **74**, 1269-1314 (1948)

[8] F. Bleich, C.B. McCullough, R. Rosecrans, G.S. Vincent, *The Mathematical theory of vibration in suspension bridges*, U.S. Dept. of Commerce, Bureau of Public Roads, Washington D.C. (1950)

[9] J.M.W. Brownjohn, *Observations on non-linear dynamic characteristics of suspension bridges*, Earthquake Engineering & Structural Dynamics **23**, 1351-1367 (1994)

[10] N.J. Delatte, *Beyond failure*, ASCE Press (2009)

[11] F.B. Farquharson, *Letter to the Editor*, ENR, p.37, July 3 (1941)

[12] E. Fermi, J. Pasta, S. Ulam, *Studies of Nonlinear Problems*, Los Alamos Rpt. LA - 1940 (1955); also in *Collected Works of E. Fermi* University of Chicago Press, 1965, Vol II, p.978

[13] F.L. Freiman, N. Schlager, *Failed technology: true stories of technological disasters*, Volume 2, UXI (1995)

[14] F. Gazzola, *Nonlinearity in oscillating bridges*, preprint

[15] F. Gazzola, R. Pavani, *Blow up oscillating solutions to some nonlinear fourth order differential equations*, Nonlinear Analysis T.M.A. **74**, 6696-6711 (2011)

[16] F. Gazzola, R. Pavani, *Blow-up oscillating solutions to some nonlinear fourth order differential equations describing oscillations of suspension bridges*, IABMAS12, 6^{th} International Conference on Bridge Maintenance, Safety, Management, Resilience and Sustainability, 3089-3093, Stresa 2012, Biondini & Frangopol (Editors), Taylor & Francis Group, London (2012)

[17] F. Gazzola, R. Pavani, *Wide oscillations finite time blow up for solutions to nonlinear fourth order differential equations*, Arch. Rat. Mech. Anal. **207**, 717-752 (2013)

[18] H. Goldstein, C. Poole, J. Safko, *Classical mechanics*, 3rd Edition, Addison Wesley (2002)

[19] D. Green, W.G. Unruh, *Tacoma Bridge failure - a physical model*, Amer. J. Physics **74**, 706-716 (2006)

[20] M. Haberland, S. Hass, U. Starossek, *Robustness assessment of suspension bridges*, IABMAS12, 6^{th} International Conference on Bridge Maintenance, Safety, Management, Resilience and Sustainability, 1617-1624, Stresa 2012, Biondini & Frangopol (Editors), Taylor & Francis Group, London (2012)

[21] M. Henón, C. Heiles, *The applicability of the third integral of motion*, The Astronomical J. **69**, 449-457 (1964)

[22] T. Kawada, *History of the modern suspension bridge: solving the dilemma between economy and stiffness*, ASCE Press (2010)

[23] A. Larsen, *Aerodynamics of the Tacoma Narrows Bridge - 60 years later*, Struct. Eng. Internat. **4**, 243-248 (2000)

[24] A.C. Lazer, P.J. McKenna, *Large scale oscillatory behaviour in loaded asymmetric systems*, Ann. Inst. H. Poincaré Anal. non Lin. **4**, 243-274 (1987)

[25] A.C. Lazer, P.J. McKenna, *Large-amplitude periodic oscillations in suspension bridges: some new connections with nonlinear analysis*, SIAM Rev. **32**, 537-578 (1990)

[26] P.J. McKenna, *Torsional oscillations in suspension bridges revisited: fixing an old approximation*, Amer. Math. Monthly **106**, 1-18 (1999)

[27] P.J. McKenna, K.S. Moore, *The global structure of periodic solutions to a suspension bridge mechanical model*, IMA J. Appl. Math. **67**, 459-478 (2002)

[28] P.J. McKenna, C.Ó Tuama, *Large torsional oscillations in suspension bridges visited again: vertical forcing creates torsional response*, Amer. Math. Monthly **108**, 738-745 (2001)

[29] J. Melan, *Theory of arches and suspension bridges*, Myron Clark Publ. Comp. (1913)

[30] K.S. Moore, *Large torsional oscillations in a suspension bridge: multiple periodic solutions to a nonlinear wave equation*, SIAM J. Math. Anal. **33**, 1411-1429 (2002)

[31] C.L. Navier, *Mémoire sur les ponts suspendus*, Imprimerie Royale, Paris (1823)

[32] New York Times, *Big Tacoma Bridge crashes 190 feet into Puget Sound*, November 8, 1940

[33] New York Times, *A great bridge falls*, November 9, 1940

[34] W. Reid, *A short account of the failure of a part of the Brighton Chain Pier, in the gale of the 30th of November 1836*, Papers on Subjects Connected with the Duties of the Corps of Royal Engineers (Professional Papers of the Corps of Royal Engineers), Vol. I (1844)

[35] Y. Rocard, *Dynamic instability: automobiles, aircraft, suspension bridges*, Crosby Lockwood, London (1957)

[36] K. Sanderson, *Millennium bridge wobble explained*, Nature, Published online 17 December 2008, doi:10.1038/news.2008.1311

[37] R.H. Scanlan, *Developments in low-speed aeroelasticity in the civil engineering field*, AIAA Journal **20**, 839-844 (1982)

[38] R.H. Scanlan, J.J. Tomko, *Airfoil and bridge deck flutter derivatives*, J. Eng. Mech. **97**, 1717-1737 (1971)

[39] R. Scott, *In the wake of Tacoma. Suspension bridges and the quest for aerodynamic stability*, ASCE Press (2001)

[40] F.C. Smith, G.S. Vincent, *Aerodynamic stability of suspension bridges: with special reference to the Tacoma Narrows Bridge, Part II: Mathematical analysis*, Investigation conducted by the Structural Research Laboratory, University of Washington - Seattle: University of Washington Press (1950)

[41] D.B. Steinman, *Letter to the editor*, ENR, 59-41, August 14 (1941)

[42] D.B. Steinman, *Design of bridges against wind: IV, Aerodynamic instability - prevention and cure*, Civil Engineers ASCE, 20-23 (1946)

[43] D.B. Steinman, S.R. Watson, *Bridges and their builders*, Second Edition, Dover, New York (1957)

[44] Tacoma Narrows Bridge collapse, http://www.youtube.com/watch?v=3mclp9QmCGs

[45] C. Truesdell, *Some challenges offered to analysis by rational thermomechanics*, In: Contemporary developments in continuum mechanics and partial differential equations, 495-603, G.M. de la Penha & L.A. Medeiros (Editors), North-Holland, Amsterdam (1978)

[46] T. von Kármán, L. Edson, *The wind and beyond, Theodore von Kármán, pioneer in aviation and pathfinder in space*, Little Brown, Boston (1967)